HADLEY CENTRE TECHNICAL NOTE NO. 6

A REVIEW OF RECENT STUDIES OF THE INFLUENCE OF SOLAR CHANGES ON THE EARTH'S CLIMATE

by

R.G.Harrison and K.P.Shine

Department of Meteorology, University of Reading
Early Gate, Reading RG6 6BB, UK

This review is prepared under contract with the Meteorological Office/Hadley Centre under the Department of the Environment, Transport and Regions Climate Prediction Programme

March 1999

Hadley Centre for Climate Prediction and Research
Meteorological Office
London Road
Bracknell
Berkshire RG12 2SY

NOTE: This paper has not been published. Permission to quote from it should be obtained from the Director of the Hadley Centre.

EXECUTIVE SUMMARY

Observed and inferred variations in total solar irradiance

- Direct satellite-based observations of the total solar irradiance (TSI – often referred to as the "Solar Constant") show with **high confidence** that the solar output is about 1 Wm^{-2} (0.08%) higher at the maximum of the 11-year solar cycle than at the minimum, for the two most recent cycles.

- Although we now have direct observations of TSI covering 2 solar cycles, these observations come from a set of 6 different satellite experiments, only a subset of which were producing data at any given time. The precision of measurements from each instruments is high and, in radiometric terms, they agree well (the spread of TSI amongst them is less than 1%). However, the level of accuracy is probably not sufficient for detecting climatically significant variations in TSI on decadal timescales. There is disagreement as to whether the TSI at the solar minima in the mid-1980s and mid-1990s was the same or not. One analysis implies a change in TSI between the two minima which would give a positive forcing equivalent to about 20% of the forcing due to increased greenhouse gas concentrations over the same period; another analysis implies little or no change.

- Several recent studies have produced time series of total solar irradiance back to the late-19th century, or before. The majority of these use recent observations of solar output to "calibrate" proxies of solar variation; they then require some measure of the change in TSI during the 17th century Maunder Minimum, when an 11-year sunspot cycle was not observed. This TSI is generally derived from observations of emissions from sun-like stars, some of which are in a non-cycling state which is presumed analogous to the Sun's Maunder Minimum

- With the exception of one of these series (which uses the variations of the Earth's surface temperature to deduce solar output changes) all these series indicate that the change in TSI since 1900 is equivalent to a radiative forcing of 0.4 Wm^{-2}; this change is roughly 20 - 25% of the change due to increases in well-mixed greenhouse gases over the same period, and is in agreement with the estimate given in IPCC (1995). However, these series disagree significantly about the details of the time evolution of the TSI, because of the use of different proxies for the TSI variation. Using a simple time-dependent zero-dimensional model of the climate, the different TSI series are shown to give a spread in the change of global-mean surface temperature, relative to 1900, of 0.2 K in the 1920s and 0.1 K in 1990.

- The biggest uncertainty in these time series of TSI is due to the lack of knowledge of the Maunder Minimum TSI. This is important because its value is used by many authors to calibrate their reconstructions of TSI variation using observed proxies (such as sunspot numbers and solar cycle length). Estimates in the literature range over an order of magnitude. However, the majority are over a smaller range indicating an uncertainty of about a factor of 2. Part of the problem is that the non-cycling stars have a wide range of emissions, so it is not possible to confidently say which of these is most appropriate for the Sun at Maunder Minimum. This implies

an uncertainty in the forcing due to changes in TSI since 1900 of about 50% either side of the 0.4 Wm^{-2} value; this uncertainty is consistent with that cited by IPCC (1995). The uncertainty in the time evolution of the TSI places strong constraints on the confidence with which "detection" and "attribution" studies can be achieved using existing series. Hence we believe that we know the absolute change in the TSI, on a century times scale with **low confidence** and the details of its time dependence with **very low confidence**.

- When century time-scale variations of TSI are included in models they can explain significant (40%) of the global-mean surface warming in the 20th century and appear to explain the rate of warming observed in the early part of the century. However, these model results are totally dependent on the quality of the TSI series that are imposed on them. Some other modelling studies have achieved equally good agreement between models and observations by excluding long term changes in solar irradiance but including the effects of volcanic aerosols. Given the uncertainties in the observed temperature variations, in the time variation of the net radiative forcing and in the climate sensitivity, it seems unlikely that a definitive and unambiguous explanation of the century time-scale variations can be achieved. Nevertheless, variations in solar output are a strong contender for explaining an appreciable fraction of this variation.

Impact of solar output changes on ozone and atmospheric circulation

- Solar-induced changes in ozone have the potential to alter the radiative forcing due to changes in TSI alone, by around 20%. However, published studies disagree on the sign of the effect of ozone changes in radiative forcing.

- General circulation model experiments which include the impact of solar-induced changes in stratospheric ozone appear to show consistent latitude-height signals in their response, which are of a size that indicates that they may be detectable in the climate record.

Variations in solar output, cosmic rays and cloudiness

- The much-publicised correlation between cosmic rays and cloudiness from the work of Svensmark and colleagues is critically examined. The "main" correlation is for a short-period of data from the International Satellite Cloud Climatology Project (ISCCP). Due to calibration problems with the ISCCP data, it is believed to be only reliable for such purposes for a short-period, 1985-1988. Hence this is only a fraction of the 11 year solar cycle. A number of studies have shown that the variation of cloudiness reported in Svensmark's work is indeed a feature of the ISCCP data, but have raised a number of issues. The cloudiness variation does not appear to have a significant impact on (at least) the solar radiation budget, the clouds do not vary systematically at different altitudes and the variation does not exist in all data sets; also much of the reported correlation occurs at times of either El Nino's or major volcanic eruptions, either of which could contribute to the cloudiness variations.

- The evidence from observations of correlations between clouds and cosmic rays

certainly does not rule out a link; however, if a link does occur, there seems as much evidence to suggest that it acts primarily via high clouds and in such a way that it will have caused a **cooling** of climate over the past century, and thus have offset the impact of increased concentrations of greenhouse gases. This is contrary to the suggestions made by Svensmark and colleagues, who have stated that the link could have contributed to a warming over the past century. However, there is **low confidence** that a significant link exists between cosmic rays and clouds, but we certainly cannot exclude the possibility.

- The possible linkage between the atmospheric electrical system and the modulation of cosmic rays allows a possible route for modulation of clouds by solar variations. But the detailed mechanism is unclear and there is much work required, some theoretical and experimental, to quantify and characterise possible processes. Mechanisms have been proposed which encourage freezing (electrofreezing) and are able to lead to substantial energy amplification of the relatively small solar fluctuations. The viability of these mechanisms depends critically on electrofreezing being experimentally established as an atmospheric process. Although there is **some evidence** to suggest that it could occur, there is no absolute evidence that it actually does occur in the atmosphere, as the definitive experiments are lacking.

1. Introduction

In order to assess the impact of human activity on climate, it is necessary to place possible human-induced changes in the context of natural variability. Natural climate variability can result from unforced "chaotic" variations and from specific causes, such as stratospheric aerosols due to explosive volcanic eruptions and changes in the solar radiation received at the Earth. This review is concerned with possible impacts of changes in solar activity on the Earth's climate over the past few centuries. It is a controversial area with a long history and has been covered in several recent reviews (e.g. IPCC 1994, 1995; NRC, 1994; Hoyt and Schatten, 1997). We will focus on recent developments in this area and cover three broad areas. Firstly, there have been several recent attempts to reconstruct the variations in the total solar irradiance ("solar constant") reaching the Earth; secondly, it has been recognised that changes in the middle atmosphere, *e.g.* via solar-induced changes in ozone, could impact on climate. Finally, and most controversially, there have been suggestions of a link between solar activity and clouds (and, hence, climate and weather).

2. Direct effect of changes in total solar irradiance

The most obvious way in which changes in solar output can impact on climate is via changes in the wavelength-integrated irradiance reaching the Earth. Following NRC (1994), and others, we refer to this irradiance as the Total Solar Irradiance (TSI), in place of the rather outmoded "solar constant". To calculate the radiative forcing resulting from a change in TSI, it is necessary to divide the solar irradiance change by 4 (the ratio of the Earth's disk as seen from the Sun to the total surface area of the Earth) and multiply by (1 - planetary albedo) to account only for that radiation which is absorbed by the Earth-atmosphere system. Taking the planetary albedo to be 0.3, and to be constant with time, a TSI change is multiplied by 0.175 to obtain the radiative forcing. There is an argument for reducing the forcing by a further factor of 0.86 to account for the fact that 14% of the changes in TSI are at ultraviolet wavelengths that do not penetrate to the troposphere (Hansen et al. 1997 and see Section 3). In order to retain comparability with earlier studies, we do not apply that factor here.

2.1 Observed changes in total solar irradiance

Since the late 1970s there has been continuous monitoring of TSI from satellites, albeit from a variety of different instruments. Although these instruments can be calibrated to a relatively high accuracy (0.2 to 0.5%) (e.g. Mecherikunnel, 1998; Fröhlich and Lean 1998a,b), this can only just resolve the variations in TSI which could be of climatic significance; fortunately, the precision/repeatability of the measurements is somewhat higher, and this permits short-term variations to be monitored with more confidence. Fröhlich and Lean (1998b) have attempted to merge the available data into a single coherent series since late 1978, by accounting for inter-satellite differences and the degradation of individual instruments. (Fröhlich and Lean (1998a) presents their method in most detail, whilst Fröhlich and Lean (1998b) presents their most up-to-date results.) Figure 2.1 shows that the unmerged data, from the satellite instruments

(acronyms are defined in the Appendix) and rocket and balloonsonde data, has a spread in TSI of around 8 Wm^{-2}. Figure 2.2 presents the merged analysis which shows the variation of about 1.2 Wm^{-2} between solar maximum and solar minimum over two solar cycles.

Fröhlich and Lean's analysis indicates that the TSI at the two minima is essentially identical. However, Willson (1997), on the basis of a comparison of the TSI at solar minima measured by two different experiments, ACRIM I and ACRIM II, suggests that the TSI had increased by about 0.036% per decade (equivalent to a radiative forcing of 0.09 $Wm^{-2}decade^{-1}$ or about 20% of the value due to well-mixed greenhouse gases), and presented supporting evidence from the ERBS instrument. Since ACRIM I and ACRIM II data did not overlap, Willson (1997) used ERB data to provide cross-calibration. Fröhlich and Lean (1998a,b) contest that such a change is not present when the data are corrected for known instrumental problems. However, the factors used by Willson (1997) to normalise ACRIM I and ACRIM II appear to agree well with independently derived values given by Crommelynck et al. (1995) (see below). This serves to emphasise that the accuracy of current TSI measurements, whilst high in radiometric terms, cannot be used to reliably determine trends that may be of climatic significance.

There have been attempts to provide reference values for the solar constant. Crommelynck et al. (1995) have derived a "Space Absolute Radiometric Reference" by using simultaneous observations of the TSI from 8 different instruments in April 1993, including shuttle-borne radiometers. The maximum difference among the sensors was only 0.16%. This reference was used by Fröhlich and Lean (1998a, b) to produce their series. The data of Crommelynck et al. (1995) also allowed adjustment factors to be derived for different instruments, to place them on a common scale. Mecherikunnel (1998) has, on the basis of measurements from ACRIM I on dates of near-zero sun-spot activity, recommended a solar minimum value of 1367 Wm^{-2}. This is somewhat higher than the minimum derived by Fröhlich and Lean (see Figure 2.2) but, using the correction factors of Crommelynck et al., the agreement is much better (and close to 1365 Wm^{-2}).

2.2 Reconstructions of century-scale variations in total solar irradiance

2.2.1 Comparison of recent reconstructions

To reconstruct the changes in TSI prior to the period of the direct observations discussed in Section 2.1, it is necessary to use some proxy of changes in solar output, such as sunspot number, normally in conjunction with recent observations of TSI. We have obtained the results from 5 recent reconstructions which take into account not only the change in solar output due to photospheric ("surface") features, such as sunspots and faculae, but also changes in the background emission from the photosphere. Two of these are from Solanki and Fligge (1998), one is an update of Lean et al. (1995b), one is an update of Hoyt and Schatten (1993) and the final one is from Reid (1997). The "raw" TSI series are shown in Figure 2.3. The series diverge in their estimates of the present day TSI by around 5 Wm^{-2}; as was discussed in Section 2.1, there have been attempts to obtain an absolute calibration of the present day TSI. It is the radiative forcing which is of most interest here. Figure 2.4 presents the

radiative forcing, relative to an arbitrary reference year (chosen as 1900) for the 5 series for the period since 1600 (in Figure 2.4 a) and for the period since 1900 (Figure 2.4 b). The forcing between 1900 and the present day (see Figure 2.4 b) is, perhaps surprisingly, very similar for 4 of these series (about 0.4 Wm^{-2} averaged over the most recent cycles), although the actual time variation over this period differs amongst the sets. These sets also imply that the solar output was roughly constant throughout the latter half of the 19th century. Hence, from these four sets, the forcing is in the range given in IPCC (1995) of 0.3 ± 0.2 Wm^{-2} since 1850. Reid's (1997) reconstruction is significantly different, with much larger changes.

To obtain a *crude* indication of the consequences of the differences between these series on global-mean surface temperature, we have used them to integrate the simple equation for global-mean surface temperature changes, ΔT, such that

$$C_s \frac{d\Delta T}{dt} = \Delta F - \lambda \Delta T$$

where C_s is the heat capacity of the surface, t is time, λ the climate sensitivity parameter and ΔF the radiative forcing. C_s was assumed to be 4 $x10^8$ J K^{-1} m^{-2}, appropriate to a planet covered by a 100 m deep mixed layer ocean, and λ was taken to be 0.67 K $(Wm^{-2})^{-1}$, appropriate to a climate sensitivity of a sensitivity of about 2.5 deg C for a doubling of carbon dioxide. For each TSI series it was assumed that the climate system was in equilibrium at the beginning of the series. The results are shown in Figure 2.5 both for the period since 1600 and for the period since 1850. The differences in the time evolution of each series gives a greater spread in temperature change by the present day (relative to 1900) than might be inferred from Figure 2.4a, with a spread from 0.2 to 0.3 deg C warming; particularly notable are the differences between the rates of change of temperature between 1900 and 1950. As with the forcing plots, Reid's (1997) reconstruction leads to a significantly different evolution of temperature and a larger overall change.

2.2.2 The basis of recent reconstructions

It is important to assess the methods used to derive these long term TSI series, to understand the differences between them. There are generally three steps in such reconstructions. The first step is to be able to characterise the *variability* of the solar irradiance in terms of observable proxies, such as sunspot features or the lengths of solar cycles. The second step is to estimate the *size* of the irradiance variations associated with this variability. As will be discussed below, in much of the recent work this calibration has been achieved by reference to estimates of the solar output at the time of the Maunder Minimum in the mid-17th century (an extended period with no sunspots) - this, in turn, has often been based on observations of emissions of particular spectral lines from sun-like stars. Finally, the absolute level of solar irradiance is referenced to recent observations, but, since we are most interested in *variations* in TSI, this latter step is of less importance here.

Reid's (1997) series is the one which is most obviously open to criticism as it used climatic information in its derivation. He hypothesises that TSI is linearly related to solar activity, as measured by a filtered sunspot number - the filter he chooses is a 15

point (in this case 15-year) Gaussian filter, so that this captures the variations for periods longer than the 11 year cycle. The slope of this fit is derived by assuming that the cold temperatures in the mid-17th century (which coincided with the Maunder Minimum) were purely a result of changes in solar activity. He assumes that the mid-17th century was 1 deg C colder than "modern" temperatures, and uses a simple energy-balance climate model to deduce the change in TSI that is necessary to explain the change - he derives a Maunder Minimum value of TSI of 1363.7 Wm^{-2}. It is unclear whether Reid has included the impacts of increased concentrations of greenhouse gases in this derivation of TSI - the text implies that he has, but when he presents time series of the global mean temperature since 1650, the temperature with both greenhouse gas and solar effects is 0.2 deg C warmer than that observed during the past two decades.

Whilst Reid's method is an interesting exercise, and he is candid about its limitations, its circular reasoning means that it is probably not a reliable method for deriving solar irradiance. Reid is essentially using the Earth's surface temperature as a radiometer, but it is a radiometer with an uncertain calibration, it is inadequately sampled over the period of interest, and it has almost certainly been "degraded" by changes in atmospheric composition that are themselves the subject of significant uncertainties (e.g. IPCC, 1995). Covey and Hoffert (1997) have pointed out that the estimate of the cooling at the time of the Maunder Minimum is not well known, particularly for the global mean; and he has ignored many known radiative forcing mechanisms (e.g. Rowntree (1998) is one recent illustration of the likely impact of volcanic eruptions.) To support his case, Reid presents a plot of recent observations, from the spacecraft era, compared to his parameterisation. This shown in Figure 2.6 - while Reid's relationship and the observed variations are in modest agreement, it is also clear that a line with a much lower slope, and hence a smaller change in solar constant, would also fit the satellite data

The other reconstructions presented here rely on "astrophysical" estimates of the change in solar output since the Maunder Minimum. Lean et al. (1992) derive a value for the Maunder Minimum TSI using emissions in the core of a particular calcium line (a Fraunhofer line at 393.4nm); they note that during contemporary solar minima, the emissions in this line indicate that there remains a bright network across the solar disk. If the relationship between emission in this line and solar output is calibrated using recent observations and then extrapolated to a state with no surface magnetic features, the TSI is reduced to 1.5 Wm^{-2} below recent minima. However, the observations of Sun-like stars by Baliunas and Jastrow (1990), indicate that the calcium emissions of non-cycling stars (which are assumed analogous to the Sun in the Maunder Minimum) is even lower, yielding a Maunder Minimum value of TSI which is about 2.7 Wm^{-2} (0.2%) below recent minimum, or 3.3 Wm^{-2} (0.24%) below the recent mean TSI. As pointed out by Lean (1994) there is a spread in calcium emissions from non-cycling stars which implies a spread in the Maunder Minimum value of TSI from close to the present solar minimum (0.6 Wm^{-2} below the recent mean) to in excess of 5 Wm^{-2} below the recent mean. It is noted that, on the basis of the calcium proxy, the Sun is amongst the most active of all the observed sun-like stars, so it is not clear whether the observations of the non-cycling sun-like proxies are truly representative of the Sun's behaviour. Soon et al. (1994) also use the calcium emission lines from sun-like stars to deduce that the Maunder Minimum TSI lies between about 2.7 Wm^{-2} and 9.5 Wm^{-2}

(0.2 to 0.7%) below the present day average value, with a mean of about 5.5 Wm^{-2}.

Nesme-Ribes et al. (1994), on the basis of modelling work which relates changes in solar rotation to changes in thermal energy in the Sun, estimate a Maunder Minimum value of TSI in the range 0.2 to 10% with a mean of 0.4%, giving a Maunder Minimum TSI of 5.5 Wm^{-2} below the present day. Mendoza (1997) uses estimates of observed solar radii and rotation rates and relates these to TSI and the calcium fluxes using correlative relationships derived from Sun-like stars. These are used to estimate larger changes in the TSI at the Maunder Minimum, which range from 0.37% to 1.23% below present day solar minimum, corresponding to a Maunder Minimum TSI of 5.5 Wm^{-2} to 15 Wm^{-2} below the present day mean. However, Mendoza (1997) also points out that there is evidence that, despite the absence of sunspots at this time, the Sun remained in a cycling state and, on this basis, estimates a value for the calcium fluxes which are only marginally lower than the present day solar minimum; on the basis of Lean et al.'s (1992) parameterisation, the Maunder Minimum TSI would only be about 1 to 1.5 Wm^{-2} below the present day mean, although the discrepancy between the two TSI estimates is not discussed.

In summary, there is a wide range of estimates of the Maunder Minimum TSI such that the reduction from the present day mean TSI covers almost an order of magnitude from less than 1.5 Wm^{-2} to 15 Wm^{-2}; for most authors their "mean" value lies in the range from around 3 to 5.5 Wm^{-2}. There is a heavy reliance on correlations between the Sun's behaviour and that of sun-like stars and a hint that models that include the effects of changes in solar rotation yield bigger changes.

Solanki and Fligge (1998) derive their series by separating out the TSI variations into changes in active regions, such as sunspots, and changes in the background ("quiet sun") emissions. The contribution due to active regions is calculated in a similar manner to Foukal and Lean (1990) using both sunspot areas and relative sunspot numbers, plus some other proxies, to calculate the sunspot and faculae contributions. The relationship is calibrated using data from the ACRIM instrument and hence implicitly assumes that the relationship has remained constant back to the 1870's. Figure 2.7 shows the variation due to these active regions - it differs from Foukal and Lean (1990) partly because of significant recent revisions to the time series of sunspot areas. The changes in the quiet sun emissions are much more difficult to derive - as evidence to support changes in the quiet sun, they cite Willson's (1997) work referred to in Section 2.1 and observations of Sun-like stars (e.g Baliunas and Jastrow, 1990). Two approaches are used. Approach A, following Lean et al. (1995), assumes a linear relationship between the photospheric emission and the chromospheric emission, which can be monitored by observing lines of calcium in the solar spectrum. Approach B, following Baliunas and Soon (1995) assumes that brightness is correlated with length of solar cycle. As shown in Figures 2.3 and 2.4, the overall variation over the past century is similar in both reconstructions, but the time evolution is significantly different, which impacts on the evolution of the global mean temperature (Fig. 2.5). Solanki and Fligge (1998) assume that the Maunder Minimum TSI is 4 Wm^{-2} below the present day value and suggest that a value of more than 5 Wm^{-2} would lead to a significant divergence between their model and recent satellite based observations. While recognising that a change of 2 Wm^{-2} is lower than most of the sun-like star estimates, such a value would still mean that their modelled variations would remain

consistent with the observed variations.

Lean et al. (1995b) also follow the model of Foukal and Lean (1990) to deduce the 11-year solar irradiance variations using observations of either group sunspot number or sunspot darkening. On longer time-scales they assume that the facular emission is related to the overall solar activity, which is given by the average value of the group sunspot number; the relationship is scaled to yield the 0.24% reduction in the TSI during the Maunder Minimum, compared to the present day mean, derived by Lean et al. (1992). They point out that their reconstruction is in general better agreement with the record of solar activity from cosmic-ray induced isotopes of carbon and beryllium than the Hoyt and Schatten (1993) series.

Hoyt and Schatten (1993) develop their reconstruction by considering, and then combining, a range of proxies for TSI. The variation uses the solar cycle length, the mean level of solar activity, the decay rates of each solar cycle, the equatorial rotation rate and the fraction of penumbral to umbral sunspots. To deduce the variations in TSI they use the Lean et al. (1992) estimate of the Maunder Minimum TSI, discussed above (this is more clearly stated in Hoyt and Schatten (1997) than it is in their 1993 paper) and point out that the size of their variations is dependent on this assumption. The TSI curve shown on Fig 2.3 is their "mean" curve - use of individual proxies would lead to a TSI that spreads roughly ± 1 Wm^{-2} either side of this curve. The high absolute value of TSI shown on Fig. 2.3 is due to the fact that they scale their irradiances to the Nimbus-7 HF values which, as shown in Fig. 2.1, are the highest of contemporary measurements. Fröhlich and Lean (1998b) compare their composite of satellite observations from 1979 with Hoyt and Schatten's series, and note that Hoyt and Schatten show a significant upward trend in TSI between the solar maxima in around 1980 and 1990 (of more than 0.5 Wm^{-2}) whilst their composite, and the Lean et al. (1995) set, shows no such change. They attribute this difference as being due to the fact that Hoyt and Schatten include a component related to solar cycle length. This implies that, if Fröhlich and Lean's composite is correct, the reliability of Hoyt and Schatten's series on longer time scales must be questioned as must a close relationship between TSI and solar cycle length.

The biggest hope for validation of these series of TSI is continued monitoring of the TSI in the future, which will indicate which set of proxies most nearly "predict" the actual variation in solar output.

2.3 Solar cycle length

One of the correlations with solar variations sought during the past century is that of solar cycle length (Hoyt and Schatten, 1997). This is a quantity which is more straightforward to observe than the cycle's amplitude, and has been the subject of several studies. Hoyt and Schatten (1997) summarise the substantial work of Clough (1943) from which it seems that solar cycle lengths are related to the amplitude of the cycle, and indeed that the cycle length is a suitable proxy for amplitude and can be determined by different means.

Of more recent interest is a paper by Friis-Christensen and Lassen (1991) in which a strong positive correlation between the solar cycle length (during the past century) and

land temperature anomalies in the northern hemisphere is found, after applying some filtering to the cycle length data. Friis-Christensen and Lassen (1991) did not attempt to form a quantitative link between solar cycle length and surface temperature. Two subsequent studies used energy balance climate models to explore influences on century timescale surface temperature variations. They included solar cycle length by assuming a linear relationship between forcing and cycle length and then derived the constant of proportionality by finding the best fit between model and observations. Kelly and Wigley (1992) found some support for a solar link as the fit, when greenhouse gas increases alone were considered, was improved when solar cycle length was included. However, it was unlikely that the temperature variation could be due entirely to solar variations as this required an implausibly high climate sensitivity. In a similar study, Schlesinger and Ramankutty (1992) found that the intercycle variations had contributed to temperature variations since 1856, but that greenhouse gases have produced the dominant contributions. IPCC (1994) includes an extended discussion about the pitfalls of the "fitting" methodology used in such studies.

Work by Laut and Gundermann (1998) investigated the correlation between cycle length and Northern hemisphere land temperatures, and in particular whether the analysis of Friis-Christensen and Lassen (1991) argues for or against an existing warming trend from non-solar causes. They show that the strong correlation between solar cycle length and surface temperature does not, of itself, imply the absence of a steady warming trend; they impose artificial warming and cooling trends on the observed temperature record and find correlations with solar cycle which are as strong as those that are found with the unmodified temperature series (figure 2.8).

2.4 Climate model simulations and correlations

Many studies explore the relationship between solar variations and climate (most often global or hemispheric mean surface temperature). These have been done via simple comparison or correlation of time series of TSI, or various proxies of solar activity with temperature (recent ones include Cliver et al. (1998), Solanki and Fligge (1998) and Svensmark (1998)) and via the use of simple climate model calculations (e.g.Wigley et al. (1997) and the work presented in Section 2.2). The statistically-based work is certainly suggestive of a relationship, but does not in general establish a cause-effect relationship (see particularly Section 2.3). The modelling work is essentially a "slave" to the quality of the TSI series.

The modelling study of Wigley et al. (1997) quantifies (using the TSI series of Hoyt and Schatten (1993)) the impact of including solar forcing (in addition to greenhouse gas and tropospheric aerosol forcing) by calculating the quality of fit with observed surface temperature changes and the implied climate sensitivity required to obtain that best fit. The solar forcing does lead to a slight reduction in the root mean square error and a corresponding reduction in the climate sensitivity; in particular the warming during the 1900-1940 period is better captured. Such work is certainly useful in showing that solar variations can impact on climate but they are by no means conclusive. As discussed in IPCC (1994) (Section 4.7.3) there are clear dangers in such "fitting" exercises, not least of which is the fact that there are substantial uncertainties in the time evolution of radiative forcings and usually only a subset of these are included. For example, Wigley et al. (1997) neglect the contribution of

volcanic aerosols; however, Rowntree (1998), using a similar type of model (and see other studies cited in IPCC (1994)), neglects solar variability but on including volcanic effects achieves an equally good agreement with observations, and in particular the representation of the observed 1900-1940 warming. At the present time, there are two clear, and not necessarily exclusive, natural explanations for the warming in the early part of the 20th century; consistency between the observed changes and modelled variations including solar effects is encouraging, but not conclusive.

The first reported coupled ocean-atmosphere GCM study to include the impact of century scale variations of TSI has been reported by Cubasch et al. (1997). They use the ECHAM-3 climate model forced using the Hoyt and Schatten (1993) TSI series; they present results from two model runs using different initial conditions. Cubasch et al. (1997) show a warming of 0.2±0.05K during the 20th century, broadly similar to that obtained with the simple model presented in Section 2.2. Over the past 30 years, the solar variability causes a warming of 0.16±0.09K. This can be compared with the warming, in the same model, of 0.54±0.13K due to greenhouse gas radiative forcing, and an observed warming of 0.39±0.15K. Hence, in this model, the contribution of TSI variations is certainly not negligible. The solar variation causes a century scale variation in temperature order 0.5 K. Within their model, the pattern of climate change is in better agreement with observations when greenhouse gas effects are included (particularly the long-term stratospheric cooling), rather than just solar variability.

3. Effect of solar-induced changes in the middle atmosphere on climate

The changes in solar irradiance are not evenly distributed across the solar spectrum, but are concentrated in the ultra-violet; wavelengths less than 400 nm contribute about 9% of the TSI but 32% of the variations in the TSI over a solar cycle (e.g. Lean 1989). Changes in the solar ultraviolet output have the potential to alter stratospheric ozone and hence modulate climate indirectly. Various modelling and observational studies (see e.g. Zerefos et al, 1997, Wuebbles et al., 1998, Haigh 1999 for review) have focused on the ozone changes. The observed and modelled total column ozone is between 1 and 2% higher at solar maximum than at solar minimum, although there are differences between models and observations in both the latitudinal and vertical distribution of this variation. In particular the observations imply larger changes in ozone in the lower and upper stratosphere than models; the unambiguous separation, in observations, of solar and volcanic influences in the lower stratosphere is difficult, as the data span less than 20 years, a period during which there have been two major volcanic eruptions (Haigh, 1999).

Wuebbles et al. (1998) have looked at the impact of long-term changes in solar UV by simulating, in a 2-D chemistry-transport model, the change in ozone during the Maunder Minimum, using Lean et al.'s (1995a) estimate of the UV changes at that time. Wuebbles et al. (1998) estimate that the global ozone column would have been 3% lower (relative to the present day solar output and ignoring human-induced changes in ozone). The increase in ozone since the Maunder Minimum is calculated to have caused a *negative* radiative forcing, presumably due to the fact that the computed

change peaks in the upper stratosphere. Wuebbles et al. (1998) compute that the radiative forcing since the Maunder Minimum due to this ozone change is -0.13 Wm^{-2}, which is a potentially non-negligible offset to the approximately +0.5 Wm^{-2} forcing due to direct changes in TSI over the same period.

Myhre et al. (1998) use the modelled variations in ozone due to solar cycle presented by Zerefos et al. (1997) to calculate the radiative forcing change due to the ozone change; they also find a decrease in forcing from solar maximum to solar minimum, with a magnitude of 0.02 Wm^{-2}; this can be compared with the increased forcing due to changes in TSI over a typical 11-year cycle of 0.1 to 0.2 Wm^{-2}, indicating that the ozone change offsets about 10 to 20% of the forcing due to TSI variations alone.

However, these estimates conflict in sign with that derived by Hansen et al. (1997) and that implied by Haigh (1999). Hansen et al. (1997) used a height profile based on observations of ozone change over recent solar cycles, albeit in a GCM with crude vertical resolution (only two layers between 10 and 150 mbar, where the ozone change is imposed). They derive an indirect forcing of +0.1 Wm^{-2} due to the ozone change. Haigh (1999) imposed ozone changes on a general circulation model (see details below); the energy absorbed below the troposphere, between 30°S and 30°N at least, is shown to be enhanced by the inclusion of ozone changes by about 20-30% compared to calculations with no ozone change, which is roughly consistent with the change derived by Hansen et al. (1997). This divergence in sign of the estimates is probably a result of the sensitivity of ozone forcing to the height profile of ozone change (e.g. Forster & Shine, 1997).

So far, in this review, the impact of solar changes has been characterised by the changes in absorbed radiation by the surface-troposphere system. There is also the potential for the solar changes to impact on circulation patterns, particularly when ozone changes are incorporated; the ozone changes can, via changes in temperature, potentially alter the static stability of the lower stratosphere as well as altering the propagation of planetary waves. Haigh (1999), in the most recent of a series of papers, has pursued this idea using the UGAMP GCM in "perpetual January" mode with fixed sea surface temperatures, imposing a variety of changes in solar irradiance and ozone. The pattern of response was found to consistent across a range of experiments. A typical one, for zonal mean temperature, is shown in Figure 3.1. The pattern of response was also reproduced in a simpler mechanistic model of the response of the Hadley circulation to changes in diabatic heating. During solar maximum, the Hadley Cell is found to weaken and broaden and is accompanied by poleward movement of the sub-tropical jets, leading to the bands of warming and cooling shown in Figure 3.1. Haigh (1999) suggests that if this pattern of response is robust, then it is of a size (several tenths of a degree in temperature) to allow its detection. This work is somewhat restricted by the use of perpetual January conditions, fixed SST's and a rather low top level (10 mbar); an extension of these calculations would clearly be of interest.

Although a manuscript is not yet available for citation, an abstract submitted to the Fall 1998 meeting of the American Geophysical Union by D.Shindell et al. (http://www.agu.org) reports similar GCM experiments to those of Haigh (1999). They confirm that changes in ozone and circulation act to amplify the signal due to TSI

changes alone; some of the signals (broadening of the Hadley Circulation, poleward movement of the jets) agree with Haigh (1999) although the abstract reports a strengthening rather than a weakening of the Hadley circulation at solar maximum. The difference may be due to the way the ozone changes are imposed on the model and the extent to which they alter the static stability of the tropical lower stratosphere. Shindell et al. also report that the such changes are in agreement with observations of an 11 year signal in geopotential height (e.g. Labitzke and Van Loon, 1989).

Arnold and Robinson (1998) report a different mechanism for amplifying the solar cycle. It is well-established that solar variability causes large changes in thermospheric temperatures, reaching 50-60 K at 120 km and several 100 K by 400 km. Arnold and Robinson (1998) propose that these changes are able to impact on the lower stratosphere via non-linear dynamical coupling. They use the UK Meteorological Office Stratosphere-Mesosphere Model (e.g. O'Neill and Pope, 1988) which is a mechanistic model forced with lower boundary conditions at about 300 mbar; Arnold and Robinson have raised the top level of the model to 140 km, by the inclusion of simplified representations of radiative processes above the mesopause. They represent solar variability by specifying a temperature profile, presumably above 90km, to which Newtonian relaxation occurs. They use the analytical and empirical model of Hedin (1983) which represents, amongst many other variables, the effect of changes in F10.7 cm flux (a proxy of solar variability) on temperature using a polynomial fit to sets of radar, rocket and satellite observations. Arnold and Robinson run their model using reference model atmospheres for solar maximum and solar minimum model for 60 days and present differences in wind and temperature fields at day 60. In the winter hemisphere, zonal-mean temperatures at 40 km are different by around 2 K and zonal-mean zonal winds are different by up to 10 ms^{-1}.

Arnold and Robinson's (1998) study is only suggestive. Their results are presented as "snap shots" of day 60 conditions and no attempt is made to assess the statistical significance of the changes they report; this is particularly important in the wintertime stratosphere where the atmosphere's unforced variability is large, and models are known to be sensitive to small changes. Also Arnold and Robinson (1998) impose the solar effects by imposing different temperatures for the atmosphere to relax to. Without further experiments, it is not possible to know the altitudes at which the temperature changes are having the most impact on the circulation and, indeed, whether the highly parameterised temperature changes seen in the reference climatology are themselves truly solar induced. Hence, whilst this was a useful study, it is felt that Arnold and Robinson (1998) would need to present evidence from longer runs, with more sophisticated statistical analysis and more exploration of the sensitivity of their results to the imposed forcing, to establish the plausibility of a real physical link between thermospheric changes and those in the lower atmosphere.

4. Cosmic rays, clouds and climate correlations

The close correlations between solar cycle length and surface temperatures, discussed in Section 2, have led to speculation that some other mechanisms beyond changes in the TSI are acting to amplify the climatic signal of solar change. Svensmark and Friis-Christensen (1997) have presented evidence that changes in cloudiness are correlated

with the flux of galactic cosmic rays reaching the Earth. The cosmic ray flux is modulated by the solar cycle, since, at times of high solar activity, fewer cosmic rays reach the Earth. Svensmark and Friis-Christensen (1997) argue that changes in cosmic ray flux may influence cloudiness in some way; they hypothesize a long term effect on climate, because a long-term increase in solar activity over the past few centuries will have been accompanied by a long-term decrease in the cosmic ray flux reaching the Earth. There is considerable evidence from the concentrations of radio-isotopes of beryllium and carbon that the cosmic ray flux has indeed been modulated (e.g. Lean et al., 1995b). This section will examine the strength of the empirical evidence for a link between cosmic rays and cloudiness, while Section 5 will discuss current understanding of the evidence at the microphysical level.

Svensmark and Friis-Christensen (1997) used the monthly-mean (C-2) dataset from the International Satellite Cloud Climatology Project (ISCCP) to produce variations in cloudiness over the period 1983-1990. They limited their analysis to oceans only and, as they used data derived from geostationary satellites, the analysis was further restricted to between about 60°S to 60°N. Figure 4.1 shows their main result, with the global mean cloudiness variations superimposed on one measure of cosmic ray intensity. The figure shows a 3-4% variation in cloudiness and there is clearly a good correlation with the cosmic ray flux. Svensmark and Friis-Christensen (1997) suggest that their results "indicate that there is a direct connection between cloudiness and intensity of cosmic ray radiation" although they do note that an actual microphysical explanation is lacking. They further suggest that the link between cosmic rays and climate operates on much longer time scales and hence can explain the high correlation between solar cycle length and temperature discussed in Section 2.

There are a number of concerns with their analysis. As with all correlation studies, the more philosophical question arises as to the extent to which the correlation indicates a real physical link. High correlations *can* arise by chance and it is only the high correlations that are likely to be published. Also, Svensmark and Friis-Christensen (1997) chose to correlate with cosmic ray time series but would have obtained a high correlation with the sunspot series - hence, even if there is a solar-clouds connection, it is not obvious, in the absence of evidence to the contrary, that it acts via cosmic rays. This criticism has, to some extent, been answered by Svensmark (1998) who shows that, during the period between 1980 and 1987, at least, the cloud variations track the cosmic ray time series more closely than one other measure of solar output (the 10.7 cm solar flux) (Fig. 4.2); however, the 10.7 cm solar flux does not itself always track the changes in solar output, particularly near solar minimum (e.g. Livingston, 1994).

In support of the possibility that any relationship between cloud and solar activity does not necessarily act via cosmic rays, Rind and Balachandran (1995) report idealised general circulation model experiments in which the ultra-violet irradiance was altered by ±5% (with ozone held constant); they found variations in cloudiness of order a few percent, due to changes in the static stability of the lower stratosphere. Although this ultra-violet change is larger than that observed, this work illustrates that more direct mechanisms exist for the modulation of clouds by solar activity. Further, Peter Thejll (Danish Meteorological Institute, personnel communication) has pointed out that the signal derived by Svensmark and Friis-Christensen (1997), because it is not from a global set, could arise from shifts in circulation systems, instead of modulation of the

global-mean cloudiness. Clearly such a hypothesis could be tested using a more complete cloud dataset.

Further, it is well known that the *sign* of the effect of cloud variations on the radiation budget depends on cloud height. Svensmark and Friis-Christensen (1997) present no evidence concerning the height of the variations, and hence it is not obvious that the variations even have the correct sign to explain their proposed link between cosmic rays and climate.

A clear problem is that their analysis covers only seven years, which is less than one complete solar cycle. Svensmark and Friis-Christensen (1997) and Svensmark (1998) do present evidence using other cloud climatologies (from Nimbus-7 data, from DMSP data and from the D-2 analysis from ISCCP) that extends the analysis from 1980 to 1995. Figure 4.3 presents the data, together with our annotations to make it clearer. In the unsmoothed data there is clearly significant noise, but the smoothed data appears to support the analysis from ISCCP C-2 data alone. However, since the absolute cloud amounts from these climatologies are not known, Svensmark and Friis-Christensen (1997) assumed that the individual data sets could be connected at the time of overlap, without any rescaling. The validity of this is questionable. The connection of the short-period of ISCCP D-2 data to the ISCCP C-2 set does not increase confidence, as it shows no evidence of any up-turn after the 1990 solar maximum. The DMSP data is even more ambiguous, for it is unclear how its time series has been connected with the ISCCP series. For the period of overlap with ISCCP C-2 data (1987 to 1990) the two sets do not show the same trend at all - the DMSP cloud is approximately constant, while over the same period ISCCP data drops by 2%. The post-1992 DMSP data appears to have been fairly arbitrarily placed so that it coincides with the cosmic ray curve. The Nimbus 7 data clearly shows a greater phase difference with cosmic rays than the ISCCP C-2 data. Hence, the evidence indicating a strong cosmic ray - cloud correlation is not strengthened by the addition of this extra data.

There is no question that the variations in ISCCP cloud amount identified by Svensmark and Friis-Christensen (1997) are a robust feature of the ISCCP data. The variations had already been presented by the ISCCP team (Rossow and Cairns 1995) who noted a possible association with El Nino. And both Kuang et al. (1998) and Kernthaler et al. (1999) have repeated the analysis, with broadly similar results, but each paper raises further concerns about the robustness of the cosmic ray link. Both studies draw attention to the problems in "calibrating" ISCCP data; to cross-calibrate the data from geostationary satellites, polar orbiters are used, but through the period of the C-2 dataset, three different polar orbiters are used, and clear "steps" have been identified in the data at the time of transition from one sensor to another - see e.g. Klein and Hartmann (1993). The consequence is that there is only a short period from 1985 to 1988 where the use of a single polar-orbitting satellite ensured consistent calibration. Brest et al. (1997) in particular warn about the difficulties in calibrating ISCCP. As one example of the difficulties, Brest et al. (1997) show that the drift in the NOAA 9 equator crossing time during the period 1985-1989, when the global cloud cover is apparently falling most rapidly, causes the monthly modal solar zenith angle to change by around 30°.

Kuang et al. (1998) analyse ISCCP C-2 data between 60°S and 60°N, presumably over

both land and ocean (this is not stated). In addition to cloud amount, they analyse the mean visible cloud optical depth and find that this varies approximately out of phase with the cloud amount data, with a peak to peak variation of mean optical depth of almost 1; see figure 4.4. Kuang et al. also show a time series of Total Ozone Mapping Spectrometer (TOMS) 360-380 nm reflectivity changes and show that (again see Fig 4.4) this varies little over the period 1984-1990, whereas simple radiation modelling would indicate it should vary by about 1% in response to the cloud amount changes. They state that the changes in optical depth approximately compensate for the changes in cloud amount, resulting in no change in the reflectivity. Their work would seem to indicate that the cloud amount variations leave no signal in the shortwave budget; hence, if there is an impact on the radiation budget, it would solely act via the thermal infrared (e.g. by modulating thin cirrus), in which case it would have the opposite sign to that required by Svensmark and Friis-Christensen (1997) - a long term decrease in cosmic rays would lead to less cloudiness but this would cool, rather than warm, the climate system. Kuang et al. hypothesize that there may have been a coincident increase in thin clouds and decrease of thick clouds during solar minimum, related to an increase in rainfall at times of increased cosmic rays. An alternative explanation of Kuang et al.'s compensation between cloud amount and optical depth is that this is a processing ambiguity in the ISCCP algorithms, so that sometimes "cloudiness" is assigned to cloud amount and sometimes it is assigned to cloud optical thickness.

Clearly the lack of an identifiable signal in the reflectivity data raises large question marks over the possibility of whether, even if the cosmic ray / cloud link is correct, it can have an impact on the Earth's radiation budget. A time series of Earth Radiation Budget Experiment (ERBE) data is shown in Figure 4.5. A 3% change in cloudiness, if evenly distributed in height and latitude, should lead to a change in absorbed solar radiation of 1.5 to 3 Wm^{-2}, according to the analysis of Ringer and Shine (1997) and others, with a change in the thermal infrared of the same general size (but opposite sign). (Svensmark and Friis-Christensen (1997) cite a value of 0.8 to 1.7 Wm^{-2}, but it is unclear if this refers to solar or net radiation). The 4 to 5 Wm^{-2} solar signal from the Mt Pinatubo is clearly seen in Figure 4.5; if present, the clouds signal also ought to be seen, particularly if it were at the 3 Wm^{-2} level, between 1985 and 1987. There is no hint of any systematic variation of this size in the data. (The step in the longwave signal in 1987 may, according to Allan (1998), be an artefact of a change in satellites at this time.) Although the analysis shown in Figure 4.5 is not global, the lack of a signal in the ERBE data is consistent with the TOMS data presented by Kuang et al. (1998) and argues against a significant impact of the cloud variations on the radiation budget.

Kuang et al. (1998) also investigate the degree of correlation between the ISCCP cloud variations and the El Nino Southern Oscillation (ENSO), and find, qualitatively, that the correlation with ENSO is as strong. They favour the solar cycle hypothesis on the basis of independent data from a later period reported by Menzel et al. (1997). However, the support for the cosmic ray link in Menzel et al. (1997) is, at best, ambiguous. They derive the cloud amount data using observations in the HIRS (High Resolution Infrared Sounder) 15 μm band and have constructed a 7 year record. Their record, both for total cloud cover, and total and thin cirrus is shown in Figure 4.6 along with the ISCCP cloud data. This figure serves to emphasize the subtlety of the ISCCP cloud amount change; in addition the HIRS data, as stated by Menzel et al. "does not show a similar [to ISCCP] correlation with cosmic rays". However, they do

report that the high cloud cover does show a correlation; Figure 4.7 illustrates this; the strength of the correlation depends greatly on the abrupt step during 1991, and since this period coincided with both the Mount Pinatubo eruption and an extended period of ENSO, the link with cosmic rays is at best speculative. Nevertheless, even if the link with cosmic rays is robust, the implication from Menzel et al.'s work is that since it is cirrus that is changing, the sign of the impact on climate would be such that a decrease of cosmic ray flux would cool climate, and not warm it as proposed by the Svensmark work.

Boucher (1999) has presented an analysis of cirrus cloud variations based on surface observations of cloud. The purpose of his note is to search for a cirrus signal due to increases in air traffic but, accidentally he chose to difference two periods which happened to be close to solar maximum (1987-1991) and close to solar minimum (1982-1986); he finds some indication of higher amounts of cirrus (about 2% over oceans) at solar maximum, which is the opposite sign to that implied Svensmark and Friis-Christensen (1997), although it is in general agreement with the long-term trends in cirrus reported by Kernthaler et al. (1999) using ISCCP data. Although Boucher's analysis is not of direct relevance to the solar/cloud debate, it does provide a reminder that other mechanisms may be involved in causing variations in cloud amount.

Svensmark and Friis-Christensen (1997) and Svensmark (1998) cite the work of Pudovkin and Veretenko (1995) in their support. Pudovkin and Veretenko (1995) report surface cloudiness observations from the former Soviet Union which indicate a short-term decrease in cloudiness arising from short periods of reduced cosmic rays ("Forbush Decreases" which are due to increases in the solar wind) using superposed epoch analysis. This is shown in Figures 4.8 and 4.9 both as the cloud amount variation relative to Forbush decreases and the fraction of clear and cloudy skies relative to Forbush decreases. The work provides only weak support for the Svensmark hypothesis. If the effect that Pudovkin and Veretenko (1995) is indeed a cosmic ray one, then the effect is only clear between 60° and 64°N, and they can find no evidence for an effect at 50°N. Moreover, their principal conclusion, consistent with that of Menzel et al. (1997), is that it is cirrus clouds that are responsible for the correlation.

As mentioned earlier Svensmark and Friis-Christensen (1997) present no information on the variation of clouds at different heights. Figure 4.6 shows that, during the ISCCP data period, cirrus data shows a near-monotonic increase in cloudiness during the period. This subject has been taken up in more detail by Kernthaler et al. (1998). They include geostationary and polar-orbiter data and use data from both land and ocean, unlike Svensmark and Friis-Christensen (1997). The total cloud amount variation they derive is 2%; the difference with Svensmark and Friis-Christensen (1997) (who found a 3-4% variation), they attribute to the inclusion of the polar orbiter data. However, as shown in Figure 4.10, individual cloud types do not display the same pattern, so that the variation in the total cloud amount is not due to any coherent variations at any particular level. When the high cloud is further divided, they find conflicting variations amongst cirrus and deep convective clouds and, as also found by Menzel et al. (1997), the near monotonic increase in cirrus cloud.

To conclude, there are two different strands to recent work. The first strand is that Svensmark's hypothesis is not so much that there is a link between cosmic rays and

clouds, but more specifically that the century timescale correlation between solar cycle length and surface temperature can be explained by the response of clouds to cosmic rays. For this to be correct, all the following assertions need to be correct: (i) that the ISCCP data are showing a true signal of changes in cloudiness, rather than some time-dependent bias in the data processing; (ii) that the signal is not due to some other forcing such as the El Nino – Southern Oscillation (ENSO); (iii) that if the signal is, at least in part, "solar" that it is uniquely related to cosmic rays; and (iv) that the variations in cloudiness are such that (a) they modulate the radiation budget and (b) that these modulations are of the correct sign (i.e. increased cloudiness leads to cooling). There is sufficient doubt about the answer to each of these questions that it is our belief that the Svensmark hypothesis is unlikely to be true. Table 4.1 summarises the arguments.

The second strand to these conclusions, though, is that the possibility of a significant relationship between the solar cycle and cloudiness **cannot** be ruled out. The lack of consistency between the individual satellite datasets during the 1980s and 1990s is hardly surprising given the difficulties in deriving them. Over this period there have been significant transitory events (most notably ENSO and volcanic eruptions) each of which have identifiable physical mechanisms that could alter cloudiness; hence, while the signals seen in these data certainly cannot be used to strongly support a solar-clouds link, neither can they be used to rule out a link. The more "transient" study by Pudovkin and Veretenko (1995) is more intriguing as the link with cosmic ray events is more direct. The robustness of their essentially statistical argument could be tested further, and the extension of their analysis to other sites, or to satellite data analyses, would be worthwhile.

TABLE 4.1 Comments on the different aspects of Svensmark and Friis-Christensen's mechanism

Aspect	Comments
There has been a long term (century-scale) decrease in galactic cosmic rays reaching the Earth due to increased solar activity.	**Not contentious**. Relationship between solar output and cosmic ray flux is well-observed for recent cycles and, for the longer term, there is good evidence from ice core records of cosmogenic isotopes.
Changes in cosmic rays lead to changes in cloudiness.	**Possible but unproven**. The evidence is discussed in section 5 (see especially Table 5.2).
A cosmic-ray related change in cloudiness has been observed.	**Contentious.** A variation of total cloudiness has been observed using ISCCP data which is in-phase with the cosmic ray variation. However, (i) the variation is not definitely a true geophysical signal, as it is not present in all satellite-derived cloud data sets; (ii) there are other contenders to explain observed variations (e.g. ENSO events and impacts of volcanoes); (iii) even if it is solar-related, the evidence to show that it is due to cosmic ray variations is not established.
Any reduction in cloudiness due to a reduction of cosmic rays leads to a decreased planetary albedo and, hence, a positive radiative forcing (i.e. a tendency to warm the surface).	**Contentious**. There is no evidence of a change in the Earth's shortwave radiation budget as a result of cosmic-ray induced cloudiness variations. There is more (albeit tenuous) evidence to indicate that, if there is an effect of cosmic rays, it is on cirrus clouds; in this case, a decrease in cloudiness would be expected to have a greater effect on the thermal infrared radiation budget such as to cause a negative radiative forcing.
There may have been a long-term decrease in cloudiness associated with the decreased cosmic ray flux.	**Contentious.** Even with present observing systems it is difficult to confidently identify decadal scale variations in cloudiness. There is no evidence of variations in cloudiness in phase with the solar cycle earlier than the past two 11-year cycles.

5. Cosmic rays and clouds

Although the suggested linkage between cosmic rays and climate has attracted current interest due to the correlation published in Svensmark and Friis-Christensen (1997), their work is certainly not the first to suggest that cosmic rays could influence meteorological processes, and indeed there is other work in which the detailed mechanisms are discussed. Svensmark and Friis-Christensen (1997) suggest that electrical charging of atmospheric aerosol influences the particles' efficacy as cloud nuclei, without discussing specifically the type of cloud they are considering. Suggestions for the precise process they were postulating are made in section 5.4 below. If the variations in cosmic ray ionisation lead to changes in aerosol electrification (see section 5.3 below), then there is a possible physical link, but the existence of the mechanism in the atmosphere is clearly unproven at present.

A more detailed mechanism involving ice clouds has been proposed in a series of papers [Tinsley and Dean (1991), Tinsley *et al.* (1989), Tinsley (1991, 1996a,b, 1997); Tinsley and Beard (1997, 1998); Kirkland *et al.* (1996); Tinsley *et al.* (1994)], by Brian Tinsley at Dallas. This work develops an atmospheric electrical mechanism to explain observed correlations between sunspot number and various indices of cyclone intensity. The solar-terrestrial correlations which motivated his work are those of Labitzke and van Loon (1989), and several papers of Roberts and co-workers (*e.g.* Roberts and Olson, 1973). In summary his mechanism depends on a microphysical electrical linkage between cosmic ray ionisation and latent heat release in supercooled clouds, which, it is argued, can modify mid-latitude depressions in both their intensity and trajectory.

It is probably appropriate to make some general observations on the atmospheric electrical system at this point. The vertical component of electric fields present in the atmosphere vary between fair weather electric values of typically $10^2 V.m^{-1}$ at the surface up to about $10^5 V.m^{-1}$ in thunderstorms before a lightning discharge (e.g. McGorman and Rust, 1998). Ionisation in the atmosphere occurs from three sources: radon, cosmic rays and terrestrial gamma radiation. (Chalmers, 1967), and the partitioning between the sources varies vertically. Near the surface, ionisation from turbulent transport of radon and other radioactive isotopes is important, together with gamma radiation from isotopes below the surface. Ionisation from cosmic rays is always present, comprising about 20% of the ionisation at the surface, and increases with increasing height in the atmosphere and dominates above the planetary boundary layer. The ionisation leads to the formation of ion pairs, which rapidly become hydrated in atmospheric air. The chemical difference between the species in the positive and negative ions leads to some physical asymmetries in the ion properties, and the negative ions are more mobile. Collisions between the ions and atmospheric aerosol leads to charge exchange and electrification of the aerosol, and the ion asymmetry ensures that the collisions do not lead to an average charge of zero. Local electric fields can cause further asymmetries, by depletion of one sign of ion concentration, and consequently substantial aerosol electrification.

Natural atmospheric ionisation could be of considerable importance in influencing atmospheric processes by

1 **direct** processes, such as production of new aerosol (*e.g.* sulphate) by gas-to-particle conversion (GPC) or homogeneous nucleation leading to new condensation nuclei
2 **indirect** processes, such as the modification of existing heterogeneous nucleation processes by affecting the properties of existing condensation nuclei (CN) or ice nuclei (IN)

5.1 Direct processes

Horrak *et al.*(1998) reported the spontaneous formation of nanometre sized ions in atmospheric air, from a change in the ion mobility spectrum of urban air. Observations of direct aerosol formation in unpolluted marine air (O'Dowd *et al*, 1996) and theoretical work on clustering reactions of ions (Castleman, 1982; Raes *et al*, 1986) suggest ions are sometimes critical in gas-to-particle conversion.

The chemical composition of carrier gases is important in ion-induced nucleation, and Emi et al. (1998) report laboratory experiments in which alpha particles have been shown to produce nanometre size particles in clean air containing 5ppm SO_2 and 3500ppm water vapour, although the ionisation rate is not reported. Adachi et al. (1998) report that the presence of NH_3 enhances the effect, and find particle concentrations of ~ $10^4 cm^{-3}$ with ~ 6MBq. Ionisation rates in the upper troposphere, where cosmic rays make their greatest contribution, are typically four or five orders of magnitude smaller than this. It is therefore just conceivable that the cosmic rays could be implicated in particle formation, but there are also other competing effects.

5.2 Indirect processes

5.2.1 The Tinsley mechanism

Tinsley's mechanism for solar-terrestrial coupling is suggested as having a substantial energy amplification, which exploits the relatively small amount of energy required to align a critical number of water molecules to nucleate ice. The mechanism can be summarised as consisting of the following stages:

1 Cosmic rays are particles of sufficiently high energy that they lead to ionisation of air in the troposphere.
2 The variations in the solar wind modulate the cosmic ray flux entering the earth's atmosphere in a such a way and the cosmic ray flux varies in antiphase with the sunspot number.
3 Cosmic ray ionisation variation leads to variation in electrification of atmospheric aerosol.
4 Electrification of aerosol increases its effectiveness as ice nuclei.
5 The solar-induced changes in ionisation cause, by 'electrofreezing', supercooled water in clouds to freeze.
6 The freezing process releases latent heat, which ultimately modifies the development of mid-latitude depressions.

Several general comments can be made about this mechanism. More detailed discussion of significant points is developed later.

1. Cosmic rays do lead to ionisation and above the boundary layer they are the principal source of tropospheric ionisation. The ionisation rate depends strongly on latitude of the ionisation rate, with increasing (and more variable) fluxes towards the poles (Neher, 1967).
2. Neutron fluxes, ionisation rates and air conductivity are indeed observed to vary with the sunspot cycle, certainly in the upper atmosphere, and also to a lesser extent in the troposphere (*e.g.* Gringel, 1978).
3. Atmospheric aerosol undergoes constant charge exchange with ions and it is certainly possible that a small fraction of aerosol can acquire significant transient charges (*e.g.* Clement and Harrison, 1991,1992). The mean charge on particles is a result of ion-aerosol interactions, and although the mean charge under steady-state conditions will be close to zero, there will be significant statistical fluctuations. Charged atmospheric aerosol particles are observed, but there are no observations to link the variations in charge with the solar cycle.
4. There is some laboratory evidence (see section 5.2) to suggest that charging alters the ice nucleation efficiency of aerosol. However laboratory experiments showing a clearly reproducible physical effect are lacking, although some are suggestive that this occurs. Some theoretical considerations suggest that electrical effects could encourage freezing of supercooled water. There appears to be no evidence of the process having been observed in the atmosphere.
5. It is not known if the laboratory experiments which have indicated the existence of electrofreezing are directly relevant to atmospheric processes.
6. The release of large quantities of latent heat within mid-latitude depressions is certainly capable, in principle, of modifying their development. The details of the release are important.

Central to Tinsley's mechanism is the presence in the atmosphere of electrofreezing. We now review the physical nature of this effect, and the experimental work supporting it.

5.2.2 Electrofreezing

Electrofreezing is a term used inconsistently in the literature. Here we will use it generally to describe the electrical-enhancement of the phase transition between supercooled water and ice. However the term is used by different authors to describe different processes (Dawson and Cardell, 1973), and to be more specific it is useful to distinguish between the different mechanisms which have been suggested.

- In *Field-Induced Electrofreezing* (FIE), a (usually large) electric field causes the freezing of a supercooled water drop. A significant series of experiments is described by Smith *et al.*(1971), in which they suggest that the effect they observed was due to mechanical disruption of the drop by the large fields, and that this disruption was the direct cause of the freezing rather than a direct electrical interaction with the water molecules comprising the drop.

- *Charge-enhanced contact nucleation* (CECN) has also been described as electrofreezing. Pruppacher (1973) describes experiments in which micron-diameter sulphur particles (which usually acted as poor ice nuclei, hardly inducing freezing at all above –20°C) were able to cause ice formation at -8°C. Pruppacher suggested this was due to negative electrification of the sulphur particles.

- *Electrically-enhanced nuclei scavenging* (EENS) is also a possible electrofreezing mechanism. It is known that electrical charging of water drops and aerosol particles increases their collision efficiency (Pruppacher and Klett, 1997), and therefore the rate at which interactions between supercooled drops and aerosol would occur. Only a small fraction of atmospheric aerosol particles are capable of acting as ice nuclei, but the increased capture probabilities would also increase the capture rate of the rare aerosol particles which are suitable ice nuclei.

- *Electrically enhanced aerosol-droplet disruption* (EEADD) is strongly related to EENS and would be hard to distinguish from it in practice. The electrically-modified collision rates could alter the closing speed of the droplet and aerosol, causing freezing by enhanced disruption at the droplet surface.

5.2.3 Studies suggesting the existence of electrofreezing

It is worthwhile to make some basic observations based on energy considerations about freezing. For freezing to occur, some initial ice-like alignment of water molecules from the liquid phase is necessary, and this structure then propagates through the supercooled drop as freezing. Latent heat is released when freezing occurs. It may be that only a small change of energy is required to cause the initial alignment of molecules, such as that caused by the presence of a particle (contact nucleation), a mechanical interaction (disruption), and that this could be supplied by electrical interactions.
There are some elementary energy calculations which are instructive. The change in free energy associated with a droplet condensing on an ion includes a thermodynamic term (which varies with supersaturation), a surface tension term and an electrical term based on the charge on the ion. A simple approach is to calculate when the electrical energy is comparable with the mechanical energy, which, for a particle of radius r allows the calculation of the number of charges j required (perhaps supplied by a colliding particle). Table 5.1 shows such a calculation, and suggest what quantity of charge is typically necessary to make mechanical changes to a particle although for very small particles surface tension is not well defined.

Table 5.1 Number of electronic charges required on a water particle of a specified radius for the electrical energy of the particle to equal its surface tension

Particle radius	Number of electronic charges
1nm	3
10nm	89
100nm	2806

The electrically-induced nucleation suggested of ice is very uncertain to estimate, in the absence of a mechanism. An indication of the energy required to initiate freezing in a supercooled droplet is to assumethat all the water molecules have to be aligned and to calculate the energy required from the polarisability and compare it with the thermal energy *i.e.* when

$$k_B T = \alpha_p E^2$$

where α_p is the polarisability of water and E is the electric field induced by the charge obtained by collision with a charged aerosol particle. For a 10 micron water drop this requires $j = 40$, and for a 1mm drop $j = 4\text{x}10^7$.

As discussed later, typical atmospheric aerosol charges are on average a few electronic charges, although the possibility exists of rare particles carrying up to an order of magnitude more charge transiently. Given the large charges required in both these calculations, if electrofreezing does occur it is more likely to affect small droplets (micron size) rather than drops.

There are different studies which have purported to study electrofreezing, which suggest the different classifications made in section 5.2.2. Some of the laboratory studies are briefly reviewed here.

In Smith *et al.*(1971) supercooled water drops of radius 2mm were passed through a region of intense electric field (up to 1.2MV.m^{-1}), and induced freezing was observed. It was suggested to be a result of cavitation and it was also suggested that the work was possibly relevant to the freezing of supercooled water in thunderstorms. Sufficiently intense electric fields would otherwise not be present in the atmosphere.

The experiment of Pruppacher (1973) mentioned above is in many ways rather important. This work strongly suggested that electrification of particles was a neglected but significant factor in enhancing particle ice nucleation efficiencies. However the fact that the sulphurous particles were charged was inferred and not observed directly, although there is little reason to doubt this conclusion. Strictly, Pruppacher's words are: 'One is therefore tempted to attribute the excellent ice nucleability of sulfur particles on contact with supercooled water drops to an electric effect'.

Katz (1968) showed that CuS (Covellite) (with diameters principally around 2micron) either charged or uncharged (having been neutralised by exposure to a Po-210 alpha source) showed very similar ice nucleating activities. But a differently prepared 'pure' CuS sample showed an order of magnitude lower activities. The preparation or purity of samples in such experiments is therefore of importance.

Adzhiev and Kalov (1996) suggest that the efficacy of AgI as an ice nucleus could be partly influenced by electrification occurring in its dispersal. Their measurements show that the AgI dispersal leads to positive electrification, proportional to the square of the radius of the droplets produced.

Abbas and Latham (1969) pursued a set of different experiments designed to compare the effect of different provocation processes causing freezing, and determined their probabilities across a set of trials (figure 5.1). Electric sparks were the most effective method, guaranteeing nucleation for droplets colder than -12°C, but there was a quantitative difference for mechanical disruption using a charged and uncharged nylon rod. The charged rod doubled the freezing probability associated with the uncharged nylon rod. An electric field (up to $1.5MV.m^{-1}$) was also able to cause freezing, but it was observed that such intense fields were unlikely to be common in the atmosphere.

Gabarashvili and Gliki (1967) showed that the effect of electric potentials on crystals of cholesterol and naphthalene was dramatic in altering their ice nucleation abilities. Using photographic observations, their work clearly showed that crystals carrying negative potentials (typically -3kV) showed remarkable ice forming capabilities when compared with positive potentials of comparable magnitude. In a later paper (Gabarashvili and Kartsivadze, 1968), work is described in which calculations show that the fields are not sufficient to be directly affecting the surface on which it forms.

Braslavksy and Lipson (1998) describe miniature apparatus in which Field Induced Electrofreezing could be routinely induced with a bulk of water. Substantial fields are applied, which correspond to about $1GV.m^{-1}$ at the atomic level.

5.2.4 Possible electrically-enhanced activation of ice nuclei

The nature of ice nuclei (IN) is a subject which has received significant attention, but as a study leaves many questions unanswered (Mason 1971, Pruppacher and Klett, 1997). Only a small fraction of aerosol particles (AP) is capable of acting as IN, and this is usually explained in terms of a chemical or shape effect, depending on the precise nucleation mechanism considered. The concentration of IN show diurnal variations (*e.g.* Rosinski *et al*, 1995), some of which have their origin as cloud condensation nuclei (Rosinski, 1995). Figure 5.2 shows the activation of different IN substances as a function of temperature.

Much of the early work on ice nucleation (Fletcher, 1966) suggests that typical IN concentrations are between 10^{-3} and 1 per litre below -20degC, rising by several orders of magnitude at temperatures between -20 and -35degC. Although there appear to be grossly inadequate IN concentrations to account for the amount of ice observed, ice multiplication mechanisms (where splintering occurs with ice formation leading) will certainly contribute to ice formation at the lower temperatures (-3 to -8degC) (Mossop, 1985).

The work of Pruppacher (1973), and to a lesser extent that of Gabarashvili and Gliki (1967) strongly suggest that aerosol electrification could lead to ice nucleation by the CECN process. The work of Katz (1968) however also emphasises that trace impurities or physical differences could be an important confounding factor. It remains therefore of great interest to establish if highly charged aerosol particles exist in the atmosphere.

5.3 Atmospheric electrification

5.3.1 Aerosol charging

In fair weather conditions, charge present in the air is partitioned between atmospheric small ions and aerosol particles, between which there are interactions. Atmospheric small ions of both signs with number concentrations n_+ and n_- are governed by

$$\frac{dn_{\pm}}{dt} = q - \alpha n_{\pm} n_{\mp} - n_{\pm} \int_{r=0}^{\infty} \sum_{j=-\infty}^{\infty} \beta_{\pm 1,j}(r) N_j(r) dr \qquad (5.1)$$

where the ions are produced at a rate q per unit volume. Ions (which are assumed to carry unit charges) are removed by ion-ion recombination (with recombination coefficient α), and by attachment to aerosol particles, which causes charge transfer to the aerosol. The aerosol attachment rate $\beta_{\pm 1,j}(r)$ depends on aerosol particle radius r and the number of elementary charges j present on the aerosol particle of radius r (e.g. Gunn, 1954). In equation (5.1), the size and charge distributions of atmospheric aerosol particles are accounted for by the integral of number concentration $N(r)$ over all particle radii, and by a sum across all possible particle charges at each radius.

The instantaneous quantity of space charge (present as the combination of charged aerosol and ions) ρ is

$$\rho = e\left[n_+ - n_- + \int_{r=0}^{\infty} \sum_{j=-\infty}^{\infty} N_j(r) dr \right] \qquad (5.2),$$

where e is the magnitude of the electronic charge. Turbulent and advective transfer processes are able to transport aerosol (last term of equation 5.2) effectively in the atmosphere; however the much greater electrical mobility of the ions means that their motion is determined principally by electrical forces. Analytical approximation to equations (5.1) and (5.2) can be obtained by assuming that the aerosol is monodisperse (*i.e.* with a number concentration $Z = \int N(r) dr$), and that there is a mean number of elementary charges j_m associated with the monodisperse aerosol. In that case, equation (5.2) reduces to

$$\rho = e\left[n_+ - n_- + j_m Z \right] \qquad (5.3).$$

An approximation for j_m can be found from the modified Boltzmann charge distribution (Clement and Harrison, 1992) as

$$j_m = \frac{4\pi\varepsilon_0 rkT}{e^2} \ln\left[\frac{n_+ \mu_+}{n_- \mu_-} \right] \qquad (5.4)$$

where $\mu_{\pm}$ are the ionic mobilities, T is atmospheric temperature and k is Boltzmann's constant. This expression emphasises the importance of the asymmetry in ion properties in determining the aerosol charge and this is also true for the charge

distribution. The ion asymmetry parameter x is defined as $x = (n_+\mu_+/n_-\mu_-)$.

Charge distributions on a set of particles exposed to unequal positive and negative ions concentrations are given by the *Modified Boltzman Distribution* (Clement and Harrison, 1992).

$$\frac{Nj}{No} = x^j \frac{\sinh(\lambda j)}{\lambda j} e^{-\lambda j^2}$$

where $\lambda = \dfrac{e^2}{8\pi\varepsilon_0 rkT}$.

The mean charge varies with the ion asymmetry parameter x (the ratio of positive and negative ion concentrations and mobilities) which is very variable, especially on the boundaries of clouds. From figure 5.3, it is clear that even for values of x typical of cloudless atmospheric air ($x = 1.2$), a number concentration of $1000cm^{-3}$ could contain of order 10 particles with up to about $j = 20$, even though the mean charge for the particle population is close to zero. Charged particles on the tails of the distribution will be rapidly neutralised.

5.3.2 Particle measurements, sonde ascents and ion asymmetry

In establishing meteorological conditions under which electrofreezing could be significant, it is clearly relevant to study observations in which regions of strong particle charging (probably negatively) have been found. There are few experimental studies which have made electrical atmospheric soundings alongside meteorological observations, in conditions other than thunderstorms, although some exist. Much of these observations came from pioneering studies using early experimental technologies.

Sagalyn and Faucher (1955) made a series of horizontal transects using aircraft to determine atmospheric particle concentrations between the surface and 5000m during the summer of 1954. In almost all of the transects positive and negatively charged particles were detected, with peak concentrations of charged particles up to $2000.cm^{-3}$. Significant concentrations ($\sim 100.cm^{-3}$) of charged particles were also found in the upper regions of their transects, well above the freezing layer (figure 5.4). Although their measurements never determined the presence of positive and negative particles simultaneously, and symmetry between the positive and negative particles was assumed in their analysis, the work clearly demonstrates that charged aerosol particles commonly exist in the freezing levels of the atmosphere. It is not possible from their measurements to determine if the particles were multiply charged.

Venkiteshwaran (1958) measured electric fields and air conductivities using modified radiosondes and determined electrical properties in non-electrified cloud. He observed that the ion concentration increased with height, and found that the measuring sonde itself was susceptible to triboelectrification as it passed through cirrus. He did not measure the positive and negative ion concentration independently, and nor did Hatakeyama *etal.*(1958) in a similar study using a different design of sonde (figure 5.5). Both these studies however, illustrated the substantial changes in ion concentrations associated with the edges of clouds, where aerosol electrification might

consequently be expected, given the significance of the term x in equations (5.5) and equations (5.6).

Gringel (1978) made more recent observations, and actual reported the ion asymmetry ratio x based on temporal averaging (figs 5.6 and 5.7), but not simultaneous bipolar observations. x remained within about 20% of 1.0, but variations were found. Figure 5.8 shows the solar variation in ionisation rate also observed by Gringel(1978).

All these observations, taken with the theoretical considerations above, suggest (1) that charged particles exist in the atmosphere and (2) fluctuations in ion concentrations could lead to transiently large charges on aerosols, perhaps on the edges of clouds. Particles with large charges are likely to rapidly attract ions of opposite sign, and their mean charge will fall as a result.

5.4 Electrical enhancement of condensation nuclei

In their discussion of possible explanations for their correlation, Svensmark and Friis-Christensen (1997) suggest that calculations show enhanced collection efficiencies of charged drops and particles over uncharged drops particles. It is certainly the case that there is an effect of electrification (Pruppacher and Klett, 1997), which in some case (thunderstorms) suggest an increase in collection efficiency of up to two orders of magnitude. However in a real cloud, electrical forces are not the only ones acting, and even if they were it is not clear from Svensmark and Friis-Christensen (1997) how the increased collection efficiency would alter cloud development, especially in warm clouds. Some theoretical work (Rusanov and Kuni, 1984), indicates that the effect of polarity is important, and that negative condensation centres are more active than positive ones.

It is more plausible that the increased collision efficiency associated with charged supercooled drops will increase the likelihood of the capture of a particle able to act as a suitable ice nucleus, *i.e.* that electrical forces will increase the likelihood of 'conventional' nucleation mechanisms occurring.

5.5 Discussions and conclusions about the electrofreezing mechanism

With the background of the previous sections, it is possible to discuss Tinsley's ideas further. It is a fact that, in some experiments, the number of ice nuclei observed in clouds is insufficient to explain the amount of ice observed at the same time. There are postulated explanations for this, such as ice multiplication, poor instrument performance and increases in the homogeneous nucleation rate. Theoretical descriptions of nucleation, especially heterogeneous nucleation are, at best, uncertain. Tinsley's suggestion that electrified aerosol is a more effective nucleator than uncharged aerosol would begin to resolve the apparent IN-cloud ice discrepancy.

Tinsley's mechanism probably has sufficient energy amplification to influence some tropospheric processes, for very small variations in solar output. Ice nucleation, if it can be triggered, certainly releases substantial quantities of latent heat, figure 5.9. The mechanism seems applicable across a range of timescales, notably for transient events such as solar flares as well as for the entire solar cycle.

The philosophical structure of Tinsley's work as described by his papers is continuous and shows development of the detail rather than as *ad hoc* modifications. The general cloud physics literature lacks the key quantitative electrofreezing experiments from which his mechanism could be developed or refuted: testing the theory awaits appropriate observations. Table 5.2 summarises the state of knowledge on different aspects of the theory.

Although electrofreezing could occur in principle in any supercooled cloud, in 'warmer' clouds (-5°C to -15°C) ice multiplication processes operate and the deficiency in IN is less critical, and in 'cold' clouds (colder than -35°C) homogeneous processes are probably active. Electrofreezing might therefore be expected to be more likely in clouds in between -15°C and -35°C. The amount of aerosol charging required is substantial and Tinsley favours charging of droplets which evaporate to leave small highly charged residues. Aerosol charges of ~100*e* are suggested as required for electrofreezing, which are much greater than those found in cloud free air. However it is true that even non-convective, non-ice clouds lead to the stratification of charge, and aerosols in these regions could charge appreciably. Marine clouds probably show the greatest conductivity contrast between clear air and cloud, but it must be emphasised that all natural clouds are complicated physical systems which contain many competing processes.

In conversations, Tinsley (1998) also suggested that freezing might be associated with Rayleigh explosions (mechanical instabilities generated by extreme electrical forces), and the emitted fragments freeze; however it is unlikely that Rayleigh limit is reached even in thunderstorms. There is also likely to be a latitude effect, as emphasised in Tinsley's work, and separating low and high latitude contributions (at 50°N) is important, as the cosmic ray influence principally affects the high latitude part.

All of Tinsley's work depends critically on electrofreezing being experimentally established as an atmospheric process. There is some evidence to suggest that it could occur, but no absolute evidence that it does. If it does occur, then it is not hard to argue that many other atmospheric processes would need to be re-evaluated, although the precise effects could only be found by detailed study. Tinsley's suggested effects are all credible, but detailed modelling studies are also really needed to assess the sensitivity.

Definitive experiments from which it can be concluded that electrofreezing exists in the atmosphere appear lacking, although there appear compelling reasons for believing that electrofreezing could occur.

TABLE 5.2 Comments on the different aspects of Tinsley's mechanism

Aspect	Comments
Cosmic rays lead to ionisation of atmospheric air throughout the troposphere.	**Not contentious**. Cosmic rays do lead to ionisation and above the boundary layer are the principal source of tropospheric ionisation. The cosmic ionisation rate depends on latitude.
Variations in the solar wind modulate the cosmic ray flux in antiphase with the sunspot number.	**Not contentious**. Neutron fluxes, ionisation rates and air conductivity are observed to vary with the sunspot cycle. They show a variation with latitude, with increasing (and more variable) fluxes towards the poles.
Cosmic ray ionisation variations lead to variations in ionisation on which electrification of atmospheric aerosol depends.	**Probable**. Atmospheric aerosol always undergoes ionic charge exchange and the mean charge varies. Charged atmospheric aerosol particles are observed, but the variation with cosmic rays has not been observed.
Electrification of aerosol increases its effectiveness as ice nuclei.	**Contentious**. There is some laboratory evidence to suggest that charging alters the ice nucleation efficiency of aerosol. There is no evidence of the process having been observed in the atmosphere.
The solar-induced changes in ionisation cause, by 'electrofreezing', supercooled water in clouds to freeze.	**Possible.** If solar-modulated cosmic-electrofreezing exists at all it will only affect a subset of clouds.
The solar electrofreezing process releases latent heat, which ultimately modifies depression development.	**Possible.** Modification of depressions is, if it occurs at all, likely to be highly selective and to depend on where, and at what stage in the depression's development, the latent heat is released.

6. Suggestions for further work

We believe that the evidence reviewed in this report is sufficiently inconclusive that further work is justified. Future research would need to concentrate on four areas. Laboratory work is important to establish if possible linkages can be established in control conditions. Field work is necessary to provide parameters describing actual atmospheric conditions. Data analysis is necessary to search for possible connections between atmospheric and solar variability. And numerical modelling is essential for trying to establish quantitative links.

6.1 Laboratory experiments

There are key laboratory measurements which need to be pursued to establish if (1) electrofreezing does occur and (2) if the process is at all significant for the atmosphere. Apparatus for repeatable freezing of the same supercooled water drop has recently been described by Harrison and Lodge (1998), but the work required is essentially that of fundamental cloud physics.

6.2 Field measurements

Atmospheric experiments on ion-induced nucleation, linking aerosol measurements in clean and polluted air with electrical measurements are clearly needed as ions could be of significance in aerosol formation (Aplin *et al*, 1998, Clement and Harrison, 1996). Experiments in both clean and polluted air would seem appropriate.

However the definitive experiments required are within an atmospheric measurement campaign to look for the combination of charged aerosol, supercooled and frozen drops. One approach would be to use a modified meteorological radiosonde system to carry extra sensors and suitable atmospheric electrical instruments such as those recently developed at Reading (Harrison 1997a,b). An alternative would be to modify an ice nuclei counter such as that under development at UMIST (Saunders, 1999) to include some discrimination between charged and uncharged IN, and deploy it in a field experiment on an aircraft.

Some long-term (longer than one solar cycle) of typical aerosol charge levels in the atmosphere would help to establish whether the electrofreezing effect, if found, was likely to be a route for solar modulation of climate.

6.3 Modelling and data analysis

(i) The two most obvious areas for further work are already "in progress" at UKMO or at Imperial College. One is to include solar reconstructions in all the past climate runs. Given the variations amongst the TSI series described in this report it is important that the impact of climate of different series is examined. The second, is for an increasingly sophisticated representation of the solar-induced ozone changes within GCMs as well as a search for the GCM-implied fingerprint in the observations.

(ii) On the cosmic ray / electrofreezing side, it is possible that sensitivity runs could be

performed. The dependence of, for example, mid-latitude depression development on the proportion of ice in clouds, at a given temperature or the rate of freezing of supercooled drops could be examined. Cloud parameterisations currently in place should be able to achieve this. Since the rate of freezing is in any case poorly known, such work would have relevance beyond the impact of solar variations.

(iii) On the data analysis side, some analysis of AMIP/ERA type runs could be undertaken to see if they, without the cosmic rays or any externally imposed solar variations, can produce the kind of variations Svensmark found in ISCCP. Further analysis of ERBE data would also be possible to see if an ERB signal could be seen that is consistent with the ISCCP variations. Finally, more ISCCP D-2 data is now available, and a repeat of the analyses using the older C-2 data is necessary to see if the C-2 signals are at least robust within the ISCCP analysis system.

(iv) The analysis of Pudovkin and Veretenko (1995) of a possible link between cloudiness and Forbush decreases is intriguing and a similar analysis at other stations, particularly at the latitudes identified by that work, would be useful.

Acronyms

ACRIM I: Active Cavity Radiometer Irradiance Monitor on the Solar Maximum Mission Satellite
ACRIM II: As ACRIM I, but flown on the Upper Atmosphere Research Satellite.
ENSO: El Nino Southern Oscillation
ERBS: Solar Monitor (similar to ACRIM) on board the Earth Radiation Budget Satellite.
HIRS: High-resolution Infrared Spectrometer
HF: Hickey-Freiden Radiometer – part of the Earth Radiation Budget experiment on Nimbus 7.
ISCCP: International Satellite Cloud Climatology Project
TOMS: Total Ozone Mapping Spectrometer
TSI: Total Solar Irradiance (the "solar constant")
UGAMP: (UK) Universities' Global Atmospheric Modelling Programme
VIRGO: Variability of Solar Irradiance and Gravity Oscillations on board the Solar and Heliospheric Observatory satellite.

Acknowledgements

We thank B. Tinsley and P. Thejll for useful discussions, J.Lean, D.Hoyt, G.Reid, S.Solanki and M.Fligge for providing their series of total solar irradiance and G.Jenkins, C.Johnson and G.Myhre for comments on a draft and encouragement.

References

Abbas M.A. and Latham J. (1969) The electrofreezing of supercooled water drops. J.Met.Soc.Japan 47: 65-74

Adachi M., Ishida T., Kim T. O. and Okuyama K. (1998) Effects of NH_3 on particle formation from NO_2/H_2O/air and SO_2/H_2O/air mixtures by α-ray radiolysis. J.Aerosol.Sci. 29, S1, 58339-58340

Adzhiev A.K and Kalov R.K. (1996) Study of effect of electrical charges and electrical field on ice-forming activity of aerosol. In: Kulmala M. and Wagner P.E. (eds.) Nucleation and atmospheric aerosols 1996, Proc. 14th International Conf on nucleation and atmospheric aerosols, Helskini, Pergamon, 338-340

Allan R.P. (1998) Modelling the variability of the Earth's radiation budget. PhD Thesis, Department of Meteorology, University of Reading.

Aplin K.L. Harrison R.G. and Wilkinson S. (1998) An electrical method of urban pollution measurement. J.Aerosol Sci 29, S1, S869-870

Arnold N.F. and Robinson T.R. (1998) Solar cycle changes to planetary wave propagation and their influence on the middle atmosphere circulation. Ann Geophysicae 16:69-76

Baliunas S. and Jastrow R. (1990) Evidence for long-term brightness changes of solar-like stars. Nature 348:520-523

Baulinas S. and Soon W. (1995) Are variations in the length of the activity cycle related to changes in brightness in solar-type stars. Astrophys. J 450:896-901

Boucher O. (1999) Air traffic may increase cirrus cloudiness. Nature 397:30-31

Braslavsky I. and Lipson S.G. (1998) Electrofreezing effect and nucleation of ice crystals in free growth experiments. Al Phys Lett 72(2), 264-265

Brest C.L., Rossow W.B. and Roiter M. (1997) Update of radiance calibrations for ISCCP. J Atmos Ocean Tech 14:1091-1109

Castleman A.W. (1982) In: Schryer D.R. Heterogeneous Atmospheric Chemistry, AGU, Washington

Clement C.F. and Harrison R.G. (1991) Charge distributions on aerosols. In: Proceedings of 8th International Electrostatics Conference, Oxford, April 1991, Institute of Physics Conference Series 118, 275-280

Clement C.F. and Harrison R.G. (1992) The charging of radioactive aerosols. J. Aerosol Sci 23, 5, 481-504

Clement C.F. and Harrison R.G. (1996) Nucleation from atmospheric fluctuations. In: Kulmala M. and Wagner P.E. (eds.) Nucleation and atmospheric aerosols 1996, Proc. 14th International Conf. on nucleation and atmospheric aerosols, Helsinki, Pergamon, 216-219

Cliver E.W., Boriakoff V. and Feynman J. (1998) Solar variability and climate change: geomagnetic aa index and global surface temperature. Geophys Res Lett 25: 1035-1038

Clough H.W. (1943) The long period variations in the length of the 11-year solar period and on current variations in terrestrial phenomena. Bull. Am Met Soc. 24, 154-163

Covey C. and Hoffert M.I. (1997) The sun-climate connection: a challenge to conventional wisdom? Climatic Change 37:387-390

Crommelynck D., Fichot A., Lee III R.B. and Romero J. (1995) First realisation of the space absolute radiometric reference (SARR) during the ATLAS 2 flight period. Adv Space Res 16:17-23

Cubasch U., Voss R., Hegerl G.C., Waszkewitz J. and Crowley T.J. (1997) Simulation of the influence of solar radiation variations on the global climate with an ocean-atmosphere general circulation model. Climate Dynamics 13:757-767

Dawson GA. and Cardell GR (1973) Electrofreezing of supercooled waterdrops. J.Geophys Res 78, 36, 8864-8866

Emi H., Shintani E., Namiki N. and Otani Y. (1998) Measurement of the ion mobility distribution at a new mobility analyser with separation in axial direction to the flow. J. Aerosol. Sci. 29, 51, 51247-51248

Fletcher N.H. (1966) The Physics of rainclouds. CUP

Forster P.M.deF. and Shine K.P. (1997) Radiative forcing and temperature trends from stratospheric ozone changes. J Geophys Res 102:10841-10855

Foukal P. and Lean J. (1990) An empirical model of total solar irradiance variations between 1974 and 1988. Science 247:556-558

Friis-Christensen E. and Lassen K. (1991) Length of the solar cycle: an indicator of solar activity closely associated with climate. Science 254:698-700

Fröhlich C. and Lean J. (1998a) Total solar irradiance variations. In F-L. Deubner et al. (eds.) "New eyes to see inside the Sun and stars" 89-102, IAU

Fröhlich C. and Lean J. (1998b) The sun's total irradiance: cycles, trends and related climate change uncertainties since 1976. Geophys Res Lett 25:4377-4380

Gabarashvili T.G. and Gliki N.V. (1967) Origination of the ice phase in supercooled

water under the influence of electrically charged crystals of cholesterol and naphthalene. Izv. Atmos. and Oceanic Physics 3, 5, 570-574

Gabarashvili T.G. and Kartsivadze A.I. (1968) Influence of electric fields upon processes of ice nucleus formation. In: Proc. Int. Conf. on Cloud Physics, August 26-30 1968, Toronto, 188-193

Gringel W. (1978) Untersuchungen zur elecktrischen Luftleitfähigkeit unter Berücksichtigung der Sonnenaktivität und der Aerosolteilchenkonzentration bis 35km Höhe PhD Dissertation, Eberhard-Karls-Universität zu Tubingen

Gunn R. and Woersner R.H. (1956) Measurements of the systematic electrification of aerosols. J. Colloid. Sci. 11, 254-259

Haigh J.D. (1999) A GCM study of climate change in response to the 11-year solar cycle. Quart J Royal Meteorol Soc (to appear)

Hansen J., Sato M. and Ruedy R. (1997) Radiative forcing and climate response. J Geophys Res, 102:6831-6864

Harrison R.G. (1997a) An antenna electrometer system for atmospheric electrical measurements Rev. Sci. Instrum 68, 3, 1599-1603

Harrison R.G. (1997b) A noise-rejecting current amplifier for surface atmospheric ion flux measurements Rev. Sci. Instrum. 68, 9, 3563-3565

Harrison R.G. and Lodge B.N. (1998) A calorimeter to detect freezing in supercooled water droplets. Rev Sci Inst 69, 11, 4004-4005

Hatakeyama H., Kobayahsi J., Kitaoka T. and Uchikawa K. (1958) A radiosonde instrument for the measurement of atmospheric electricity and its flight results. In: Smith L. G.. (ed.) 1958 Recent advances in atmospheric electricity, Proc. Of 2nd Wentworth Conference, Pergamon Press, New York.

Hedin A.E. (1983) A revised thermospheric model based on mass spectrometer and incoherent scatter data: MSIS-83. J Geophys Res 88:10170-10188

Horrak U., Salm J. and Tammet H. (1998) Bursts of intermediate ions in atmospheric air. J.Geophys Res 103 D12, 13909-13915

Hoyt D.V. and Schatten K.H. (1993) A discussion of plausible solar irradiance variations, 1700-1992. J Geophys Res 98(A11):18895-18906

Hoyt D.V. and Schatten K.T. The role of the sun in climate change. OUP, 1997

IPCC (1994) Climate Change 1994. Intergovernmental Panel on Climate Change. Cambridge University Press.

IPCC (1995) Climate Change 1995. Intergovernmental Panel on Climate Change.

Cambridge University Press.

Katz U. (1968) The ice nucleation activity of electrically charged and uncharged CuS particles. In: Proc Int Conf on Cloud Physics, August 26-30 1968, Toronto, 183-187

Kelly P.M. and Wigley T.M.L. (1992) Solar cycle length, greenhouse forcing and climate change. Nature 360:328-330

Kernthaler S.C., Toumi R. and Haigh J.D. (1999) Some doubts concerning a link between cosmic ray fluxes and global cloudiness. Geophys Res Lett (provisionally accepted)

Kirkland M. W., Tinsley B. A. and Hoeksema J. T. (1996) Are stratospheric aerosols the missing link between tropospheric vorticity and Earth transits of the heliospheric current sheet? J. Geophys. Res. 101, D23, 29689-29699.

Klein S.A. and Hartmann D.L. (1993) Spurious changes in the ISCCP dataset. Geophys Res Lett 20:455-458

Kuang Z., Jiang Y. and Yung Y.L. (1998) Cloud optical thickness variations during 1983-1991: solar cycle or ENSO? Geophys Res Lett 25:1415-1417

Labitzke K. and van Loon H. (1989) Association between the 11-year solar cycle, the QBO and the atmosphere, III Aspects of the Association. J. Clim. 2, 554-565.

Laut P. and Gundermann J. (1998) Does the correlation between solar cycle lengths and Northern Hemisphere land temperatures rule out any significant global warming from greenhouse gases? J. Atmos. Solar-Terrest. Phys. 60, 1, -13

Lean J. (1989) Contribution of ultraviolet irradiance variations to changes in the Sun's total irradiance. Science 244:197-200

Lean J. (1994) Solar forcing of global change. In: Nesme-Ribes E. (ed.) 1994, The Solar Engine and its Influence on Tererestrial Atmosphere and Climate. NATO ASI Series Vol I25 Springer-Verlag Berlin.

Lean J.L., White O.R. and Skumanich A. (1995a) On the solar ultraviolet spectral irradiance during the Maunder Minimum. Global Biogeostem. Cycle, 9:171-182

Lean J., Beer J. and Bradley R. (1995b) Reconstruction of solar irradiance since 1610: Implications for climate change. Geophys Res Lett 22:3195-3198

Lean J., Skumanich A. and White O. (1992) Estimating the sun's radiative output during the Maunder Minimum. Geophys Res Lett 19:1591-1594

Livingston W. (1994) Surrogates for total solar irradiance. In: Nesme-Ribes E. (ed.) 1994, The Solar Engine and its Influence on Tererestrial Atmosphere and Climate. NATO ASI Series Vol I25 Springer-Verlag Berlin.

Mason B.J. (1971) The Physics of Clouds. OUP

McGorman D.R. and Rust W.D. (1998) The electrical nature of storms. OUP

Mecherikunnel A.T. (1998) Solar total irradiance: a reference value for solar minimum. Solar Phys 177:11-23

Mendoza B. (1997) Estimations of Maunder Minimum solar irradiance and Ca II H and K fluxes using rotation rates and diameters. Astrophys J 483:523-526

Menzel W.P., Wylie D.P. and Strabala K.I. (1997) Seven years of global cirrus cloud statistics using HIRS. In: Smith W.L. and Stamnes K. IRS 96: Current problems in Atmospheric Radiation (A Deepak Publishing) 719-725

Minnis P., Harrison E.F., Gibson G.G., Denn F.M., Doelling D.R. and Smith W.L.Jr. (1993) Radiative forcing by the eruption of Mt. Pinatubo deduced from NASA's Earth Radiation Budget Data. Science, 259:1411-1415

Mossop S.C. (1985) The origin and concentration of ice crystals in clouds. Bull.Am.Meteor.Soc 66, 264-273

Myhre G., Stordal F., Rognerud B. and Isaksen I.S.A. (1998) Radiative forcing due to stratospheric ozone. In: Bojkov R.D. and Visconti G. (Eds.) Atmospheric ozone: Proc. Of the XVIII Quadrennial Ozone Symposium. 813-816

Neher H.V. (1967) Cosmic ray particles that changed from 1954 to 1958 to 1965. J.Geophys.Res. 72, 1527-1539

Nesme-Ribes E., Solokoff D., Ribes J.C. and Kremliovsky M. (1994) The Maunder minimum and the solar dynamo. In: Nesme-Ribes E. (ed.) 1994, The Solar Engine and its Influence on Tererestrial Atmosphere and Climate. NATO ASI Series Vol I25 Springer-Verlag Berlin.

NRC (1994) Solar Influences on Global Change. National Research Council, Washington DC

O'Dowd C.D, Smith M.H., Lowe J.A., Harrison R.M., Davison B. and Hewitt C.N. (1996) New particle formation in the marine environment. In: Kulmala M. and Wagner P.E., Proc. 14th Int. Conf. on Nucleation and Atmospheric Aerosols, 925-928

O'Neill A. and Pope V.D. (1988) Simulations of linear and non-linear disturbances in the stratosphere. Quart. J. Royal Meteorol. Soc. 114:1063-1110

Pruppacher H.R (1973) Electrofreezing of supercooled water. Pure. Al Geophys. 104, 623-634

Pruppacher H.R. and Klett J.D. (1997) Microphysics of clouds and precipitation. 2nd edition, Kluwer

Pudovkin M.I. and Veretenenko S.V. (1995) Cloudiness decreases associated with Forbush-decreases of galactic cosmic rays. J Atmos Terr Phys 75:1349-1355

Raes F., Janssens A. and Van Dingenen R. (1986) The role of ion-induced aerosol formation in the lower atmosphere. J. Aerosol. Sci. 17, 3, 466-470

Reid G. (1997) Solar forcing of global climate change since the mid-17th century. Climatic Change 37:391-405

Rind D. and Balachandran N.K. (1995) Modelling the effects of UV variability and the QBO on the troposphere-stratosphere system. Part II: The tropopause. J. Clim. 8:2080-2095

Ringer M.A. and Shine K.P. (1997) Sensitivity of the Earth's radiation budget to interannual variations in cloud amount. Climate Dynamics 13: 213-222

Roberts W. O. and Olson R. H. (1973) Geomagnetic storms and wintertime 300mb trough development in the North Pacific – North American area. J. Atmos. Sci. 30, 135.

Rosinski J. (1995) Cloud condensation nuclei as a real source of ice forming nuclei in continental and marine air masses. Atmospheric Research 38, 351-359

Rosinski J., Nagamoto C.T. and Zhou M.Y. (1995) Ice forming nuclei over the East China Sea. Atmospheric Research 36, 95-105

Rossow W.B. and Cairns B. (1995) Monitoring changes of clouds. Climatic Change 31:305-347

Rowntree P.R. (1998) Global average climate forcing and temperature response since 1750. Int. J. Climatol. 18:355-377

Rusanov A.I. and Kuni F.M. (1984) Reformulation of the thermodynamic theory of nucleation on charged particles. J.Coll. Int Science 100, 1, 264-277

Sagalyn R.C. and Faucher G.A. (1955) Time variations of charged atmospheric nuclei. In: Artificial Stimulation of Rain, Proc of the 1st Conference on the Physics of cloud and precipitation particles, Woods Hole Oceanographic Institution, Massachusetts September 7-10, 1955, Pergamon Press.

Saunders C. P. R. (1999) Personal communication with R.G.Harrison.

Schlesinger M.E. and Ramankutty N. (1992) Implications for global warming of intercylcye solar irradiance variations Nature 360:330-333

Smith MH, Griffiths RF, Latham J (1971) The freezing of raindrops falling through strong electric fields. Quart J Roy Meteorol Soc 97:495-505

Solanki S.K. and Fligge M. (1998) Solar irradiance since 1874 revisited. Geophys Res Lett 25:341-344

Soon W.H., Baliunas S.L. and Zhang Q. (1994) A technique for estimating long-term variations of solar total irradiance: Preliminary estimates based on observations of the Sun and solar-type stars.. In: Nesme-Ribes E. (ed.) 1994, The Solar Engine and its Influence on Tererestrial Atmosphere and Climate. NATO ASI Series Vol I25 Springer-Verlag Berlin.

Svensmark H. (1998) Influence of cosmic rays on Earth's climate. Phys Rev Lett 81:5027-5030

Svensmark H.and Friis-Christensen E. (1997) Variations of cosmic ray flux and global cloud coverage – a missing link in solar-climate relationships. J Atmos Solar-Terrestrial Phys 59:1225-1232

Tinsley B. A. (1991) Interpretation of short-term solar variability effects in the troposphere. J. Geomag. Geoelect. 43, 775-783.

Tinsley B. A. (1996a) Evidence for cloud-climate interactions due to atmospheric electricity effects on ice nucleation. Proc. 12th Int. Conf. on Clouds and precipitation, Zurich, August 1996.

Tinsley B. A. (1996b) Correlations of atmospheric dynamics with solar wind-induced changes of air-earth current density into cloud top. J. Geophys. Res. 101, D23, 29701-29714.

Tinsley B. A. (1997) Do effects of global Atmospheric Electricity on clouds cause climate changes? EOS, Trans. A. G. U. 78, 33 (August 19th, 1997)

Tinsley B. A. and Beard K. V. (1997) Links between variations in solar activity, atmospheric conductivity and clouds: an informal workshop. Bull. Am. Met. Soc. 78, 4, 1-3.

Tinsley B. A. and Beard K. V. (1998) Solar wind Connections to Climate: Atmospheric Electricity affecting cloud microphysics, presented at AAAS meeting, Philadelphia, February 14th 1998.

Tinsley BA, Dean GW (1991) Apparent tropospheric response to MeV-GeV particle flux variations: a connection via electrofreeezing of supercooled water in high-level clouds? J Geophys Res 96:22283-22296.

Tinsley BA., Heelis RA (1993) Correlations of atmospheric dynamics with solar activity: evidence for a connection via the solar wind, atmospheric electricity and cloud microphysics. J Geophys Res 98:10375-10384.

Tinsley BA, Brown GM, Scherrer PH (1989) Solar variability influences on weather and climate: possible connections through cosmic ray-fluxes and storm intensification J Geophys Res 94:14783-14792.

Tinsley BA, Hoeksema JT, Baker DN (1994) Stratospheric volcanic aerosols and changes in air-earth current density at solar wind magnetic sector boundaries as conditions for the Wilcox tropospheric vorticity effect. J Geophys Res 99:16805-16813.

Tinsley B.A. (1998) personal communication with R.G.Harrison, September 1998

Venkiteshwaran S.P. (1958) Measurement of the electrical potential gradient and conductivity by radiosonde at Poona, India. In: Smith L. G. (ed.) 1958 Recent advances in atmospheric electricity, Proc. Of 2nd Wentworth Conference, Pergamon Press, New York.

Wigley T.M.L., Jones P.D. and Raper S.C.B. (1997) The observed global warming record: what does it tell us? Proc. Natl. Acad. Sci. USA 94:8314-8320

Willson R.C. (1997) Total solar irradiance trend during solar cycles 21 and 22. Science 277:1963-1965

Wuebbles D.J., Wei C.F. and Patten K.O. (1998) Effects on stratospheric ozone and temperature during the Maunder Minimum. Geophys. Res. Lett., 25:523-526

Zerefos C.S., Tourpali K., Bojkov B.R., Balis D.S., Rognerud B. and Isaksen I.S.A. (1997) Solar activity – total column ozone relationships: observations and model studies with heterogeneous chemistry. J. Geophys. Res. 102: 1561-1569

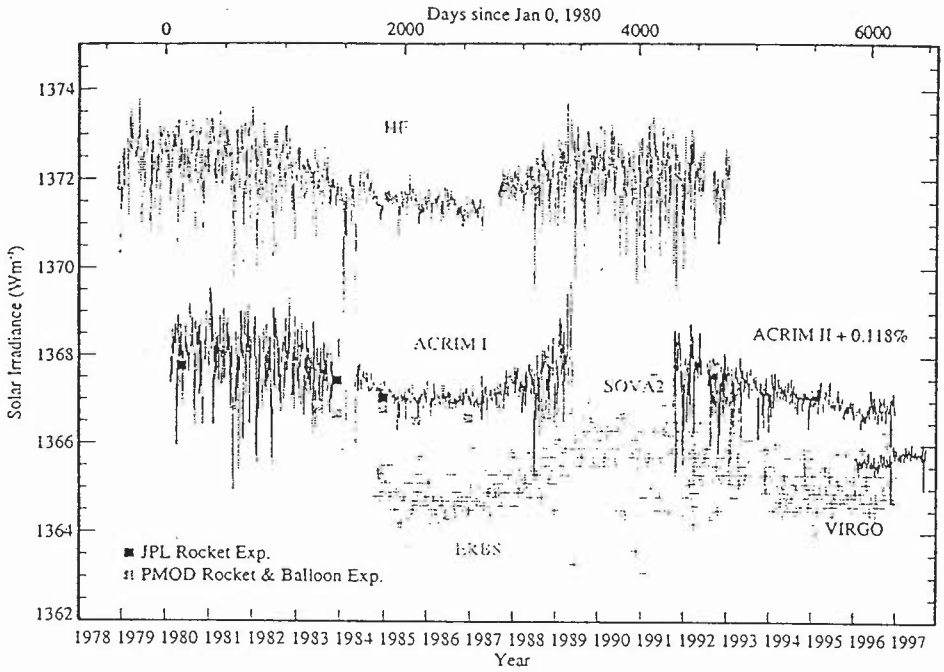

Figure 2.1 Time series of daily values of total solar irradiance in Wm^{-2} as observed by HF/ERB on NIMBUS-7, ACRIM I & II on SMM and UARS, the solar monitor on ERBS, SOVA2 on EURECA and VIRGO on SOHO. The results of the rocket and balloon experiments of JPL and PMOD/WRC are also plotted for comparison. (From Fröhlich & Lean, 1998a.)

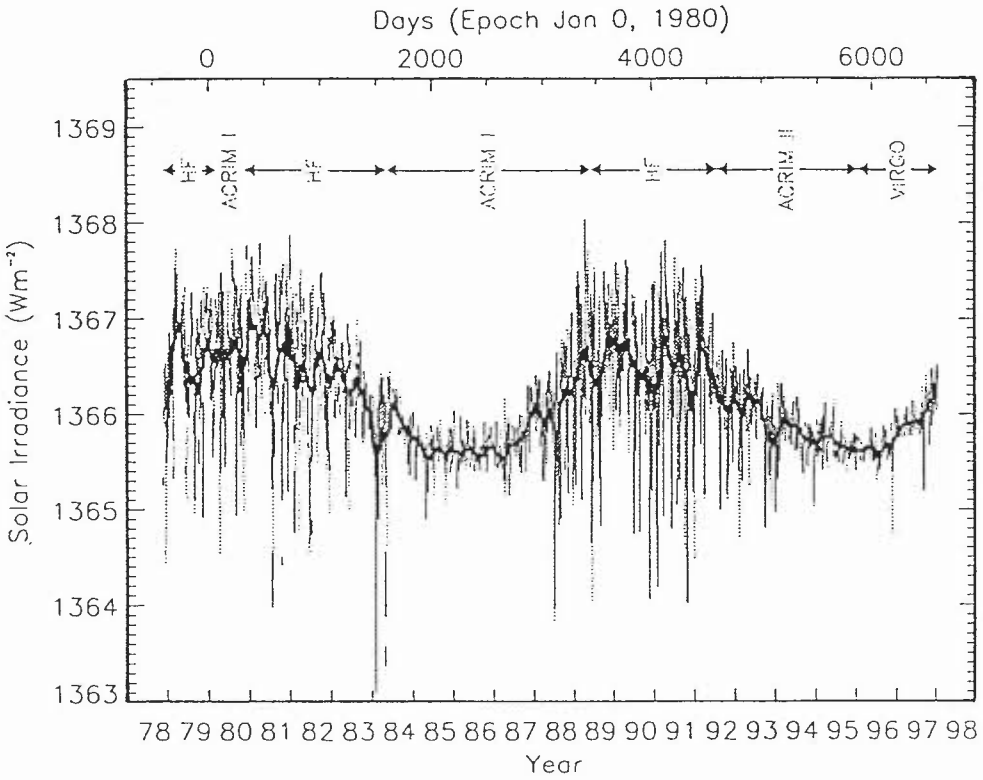

Figure 2.2 A composite record of solar total irradiance compiled from detailed cross-calibrations of various radiometric measurements from the end of 1978 to the present, and adjusted to the absolute scale of the Space Absolute Radiometric Reference. (From Fröhlich & Lean, 1998b.)

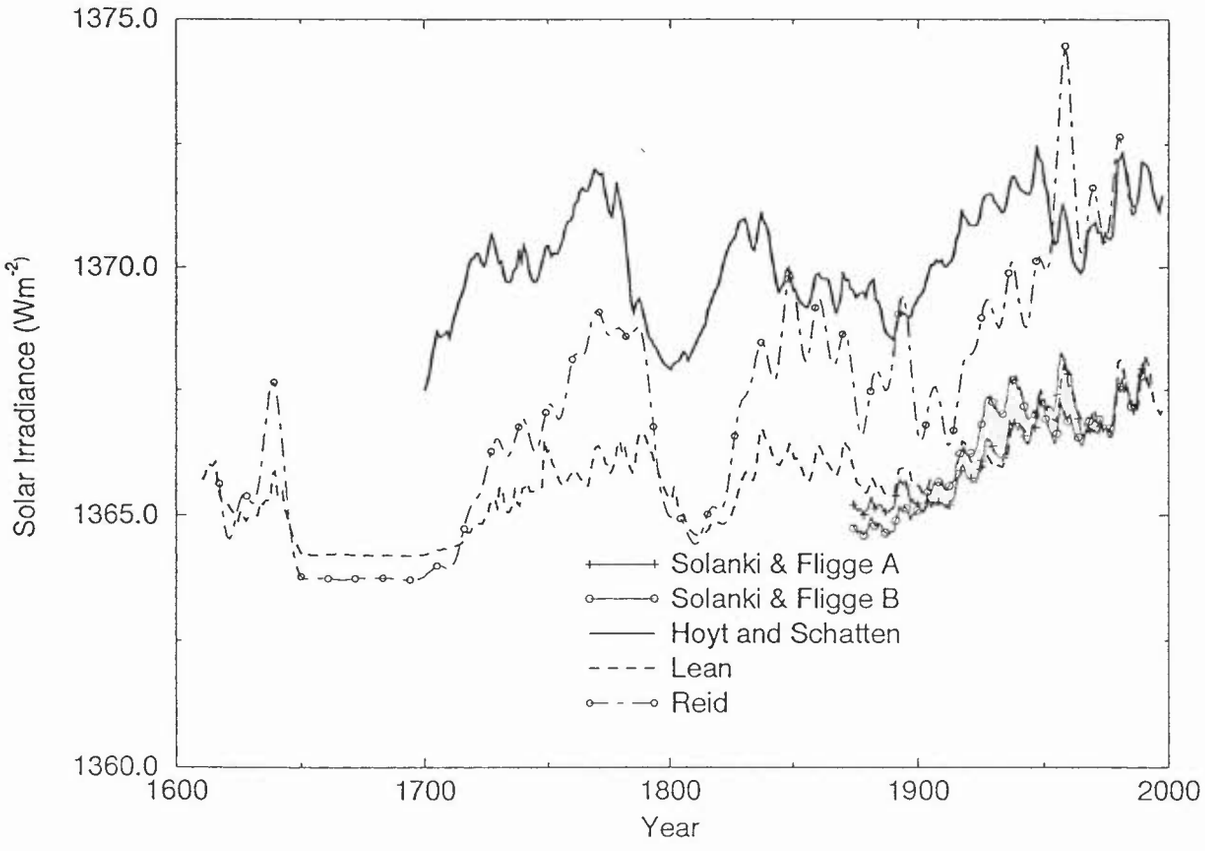

Figure 2.3 Comparison of total solar irradiance (in Wm^{-2}) time series for the period since about 1600. The series included are updated ones from Hoyt & Schatten (1993) and Lean et al. (1995b), one from Reid (1998) and two from Solanki & Fligge (1998).

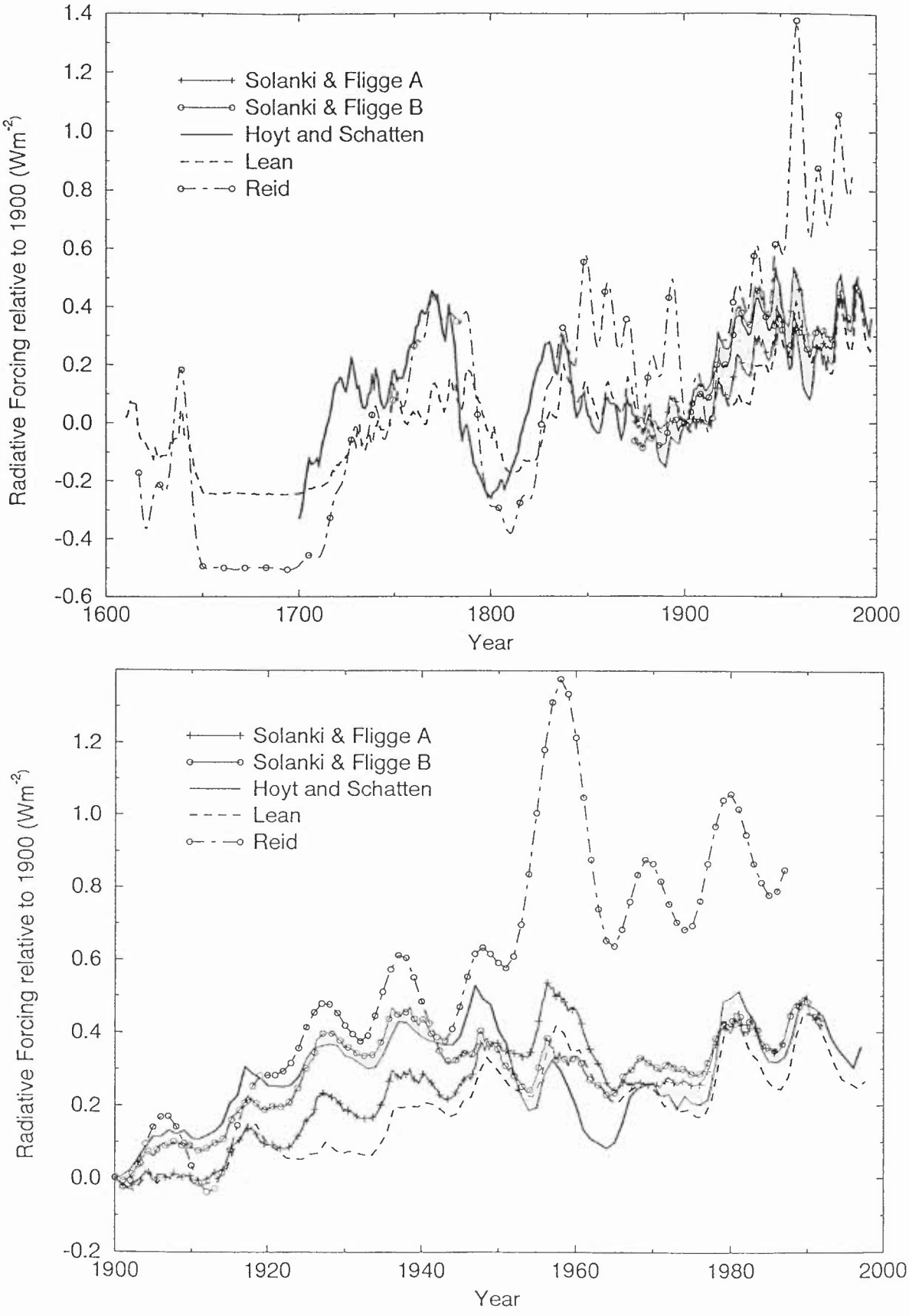

Figure 2.4 Radiative forcing (in Wm^{-2}), relative to an arbitrary reference year (1900) using the total solar irradiance time series shown in Figure 2.3. The conversion from TSI to forcing includes the geometric factor (divide by 4) and the albedo (multiply by 0.7). (a) shows the time series for the period from 1600 and (b) shows an expanded plot for the period since 1900.

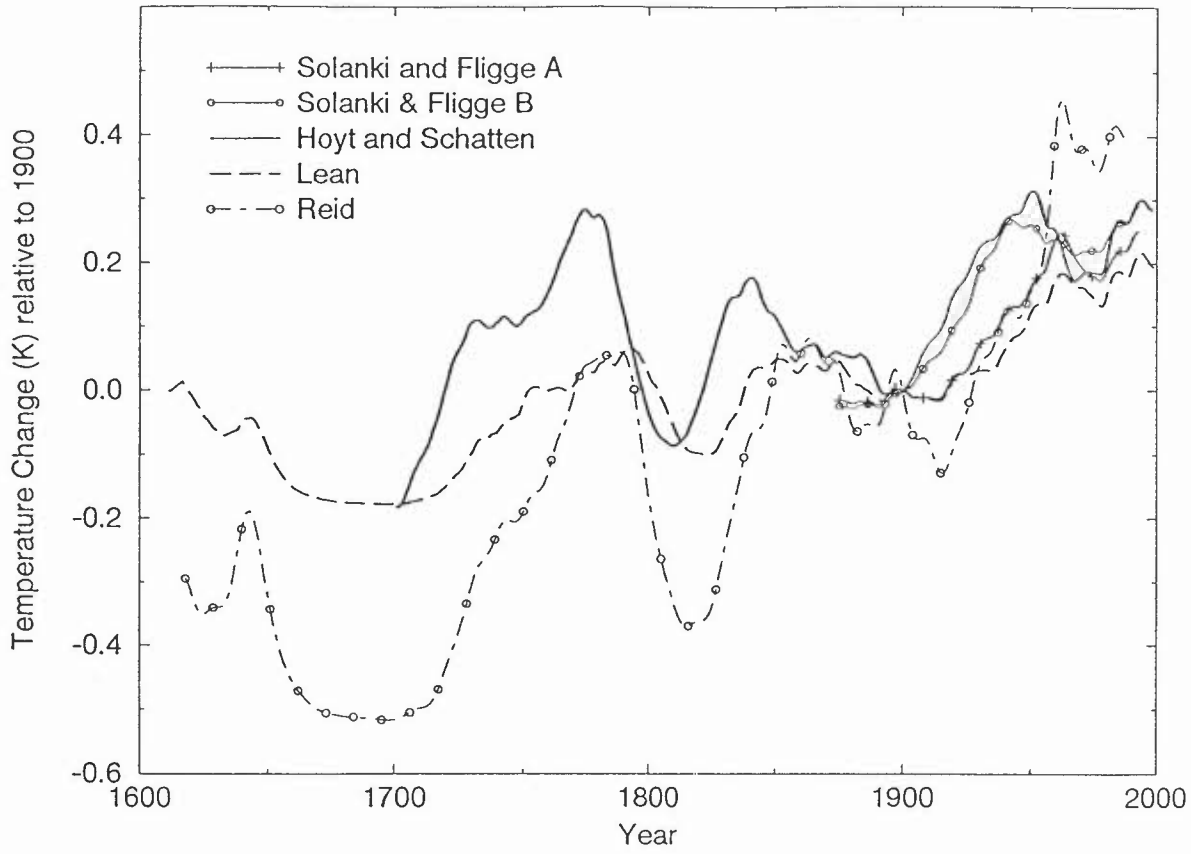

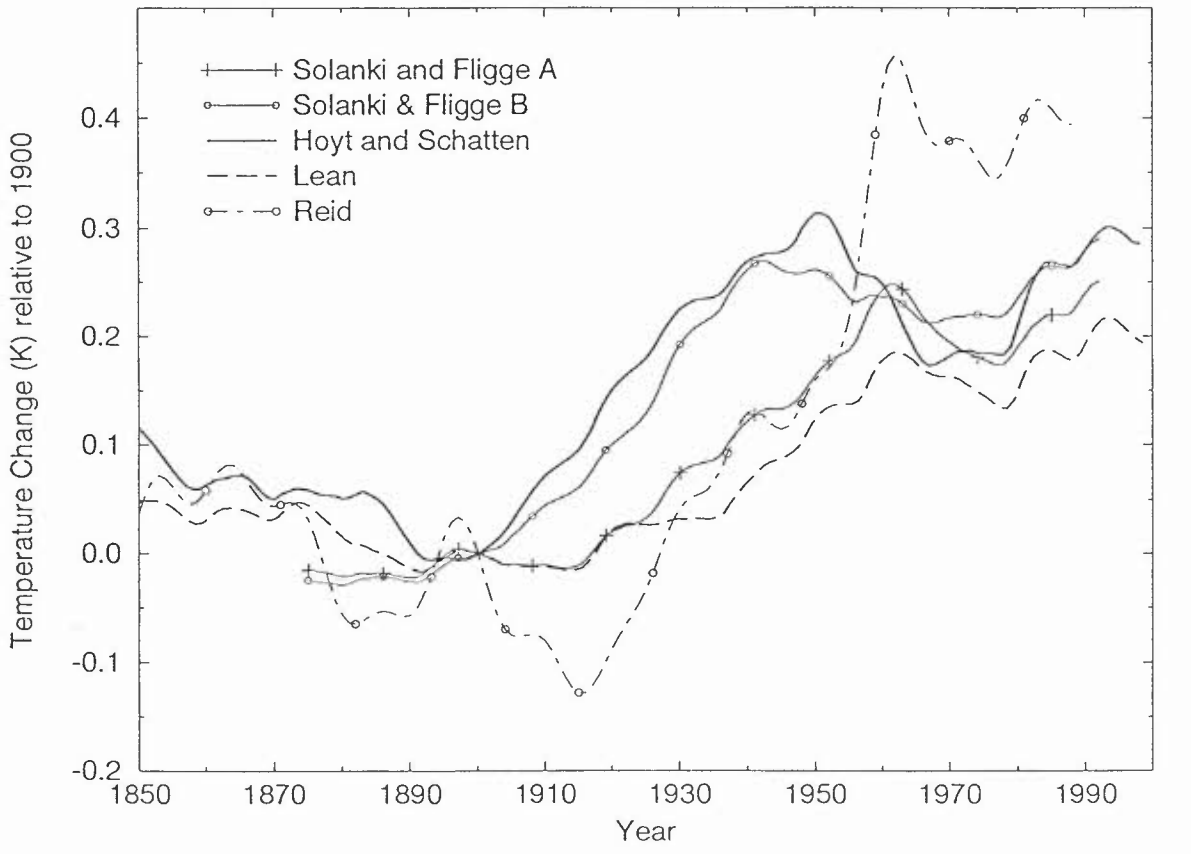

Figure 2.5 Global mean surface temperature anomaly (in K), relative to an arbitrary reference year (1900), using the radiative forcing series shown in Figure 2.4, and using a very simple global-mean climate model described in the text. The climate system is assumed to be in equilibrium at the start of each time series. (a) shows the temperatures for the period since 1600 while (b) shows an expanded plot for the period since 1850.

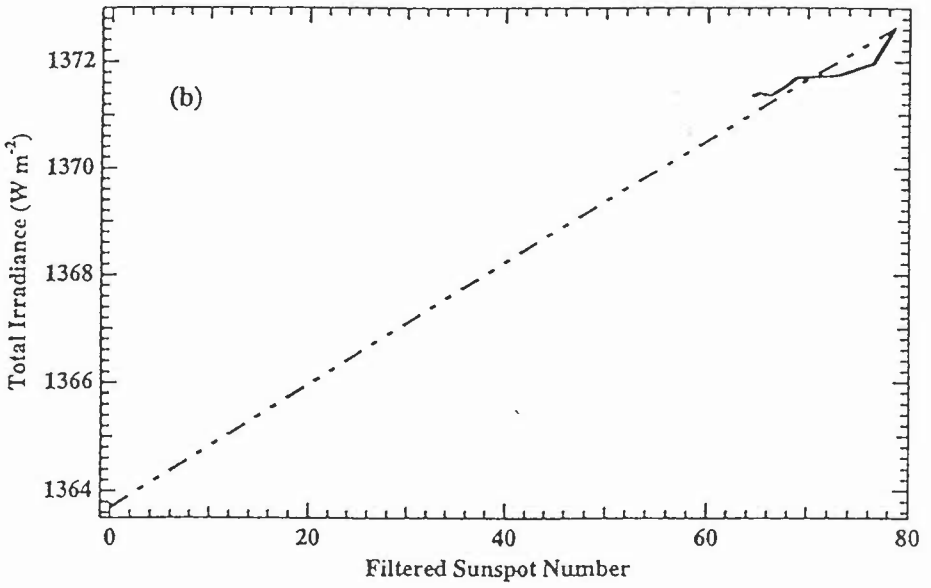

Figure 2.6 The assumed linear relationship between filtered sunspot number and total irradiance, based on the requirement that Maunder Minimum temperatures be about 1°C cooler than modern temperatures. The observed relationship in the spacecraft era is superimposed. (From Reid, 1997.)

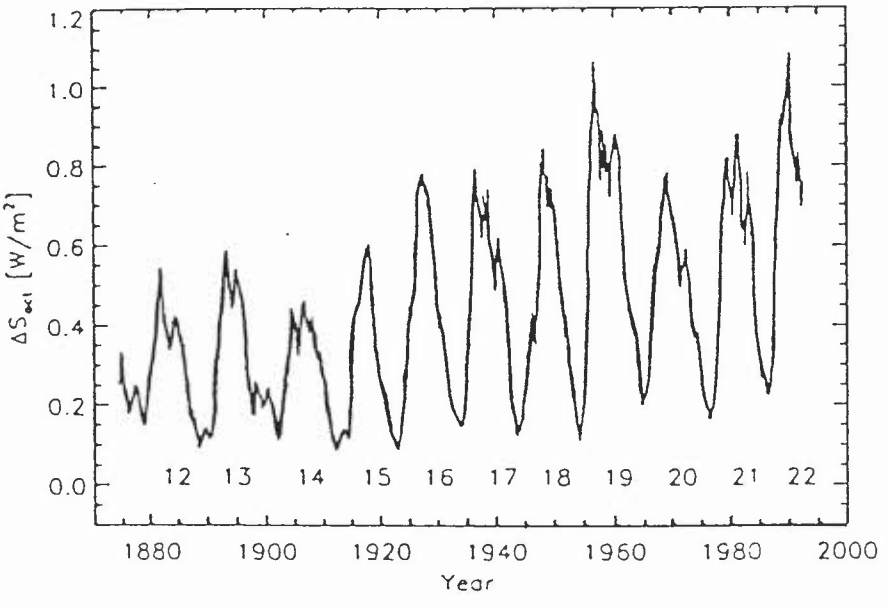

Figure 2.7 Time-dependence of reconstructed solar irradiance variations due to solar active regions, ΔS_{act}, versus time. The irradiance has been smoothed by a 1-year running mean. Data gaps have been accounted for in two different ways, by interpolating across them and by binning the data points. Both techniques give almost indistinguishable results. Solar cycle numbers are indicated. (From Solanki & Fligge, 1998.)

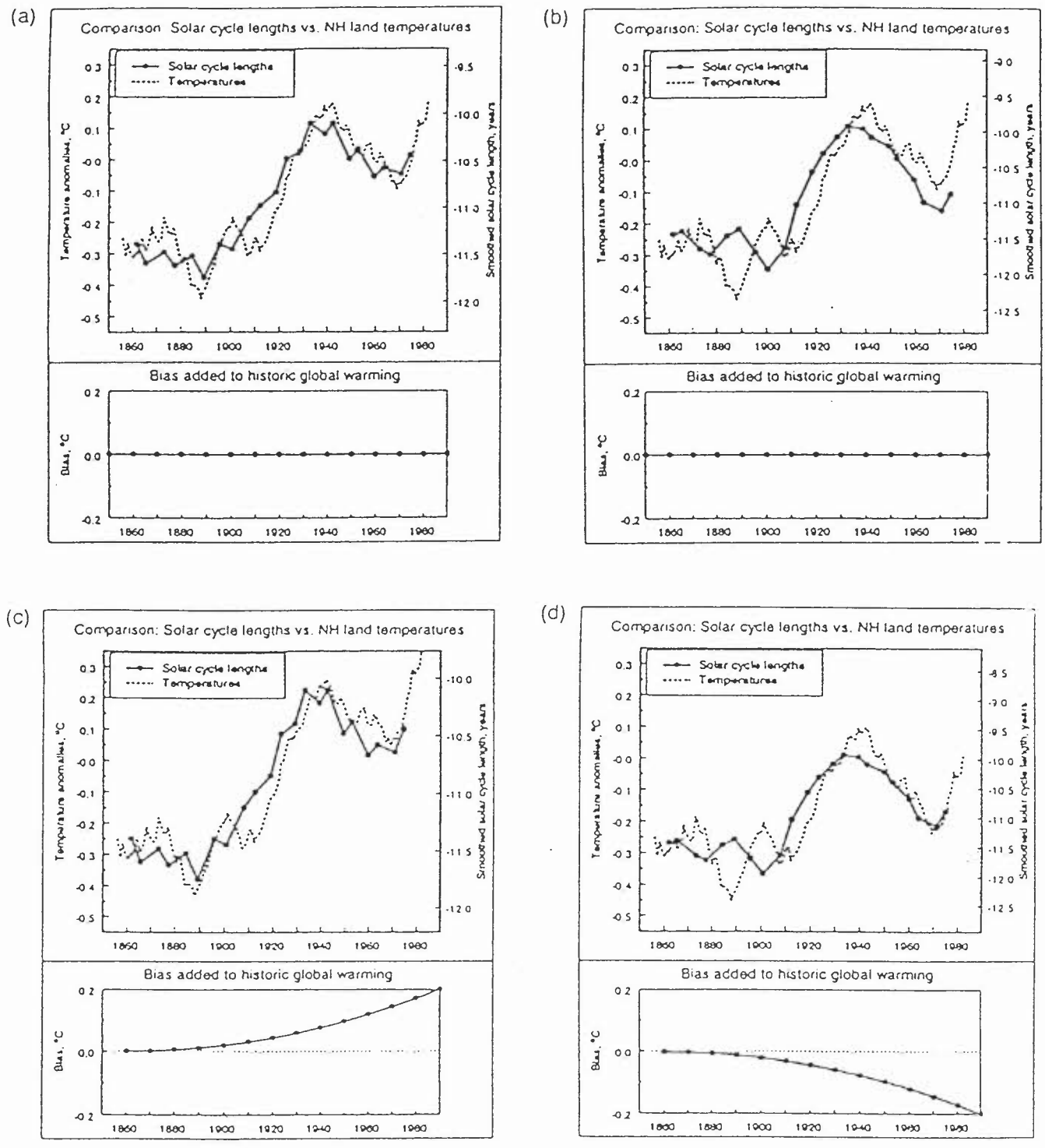

Figure 2.8 Comparison between solar cycle length and northern hemisphere land surface temperature produced by (a) a 5 term 1-2-2-2-1 filtering, (b) a 7 term binomial filtering (c) a positive bias and a 5 term 1-2-2-2-1 binomial filtering and (d) a negative bias and a 7 term binomial filtering. (From Laut and Gundermann, 1998).

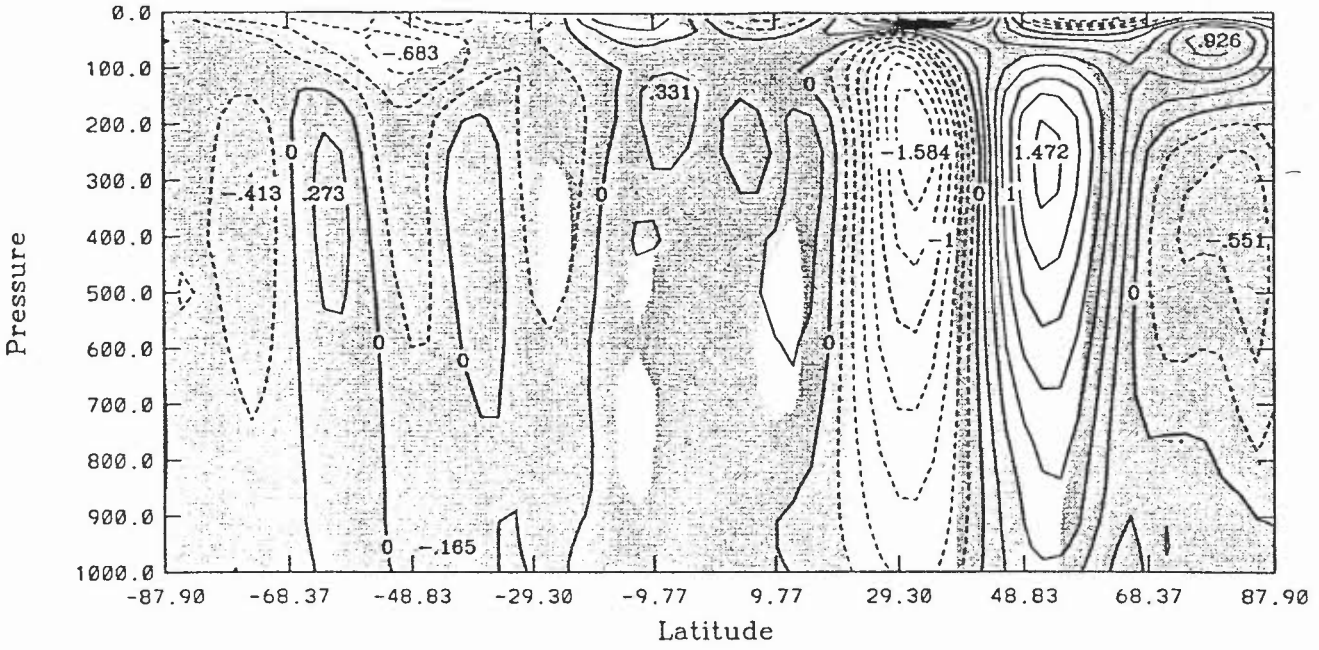

Figure 3.1 Difference in zonal mean temperature (in K) between an experiment with the UGAMP GCM in which no solar-induced ozone changes are imposed and one in which a solar-induced total column ozone change derived from TOMS observations is imposed. The model is run in perpetual January mode with fixed sea surface temperatures. Shading indicates that the difference is not statistically significant at the 95% level. (From Haigh, 1999.)

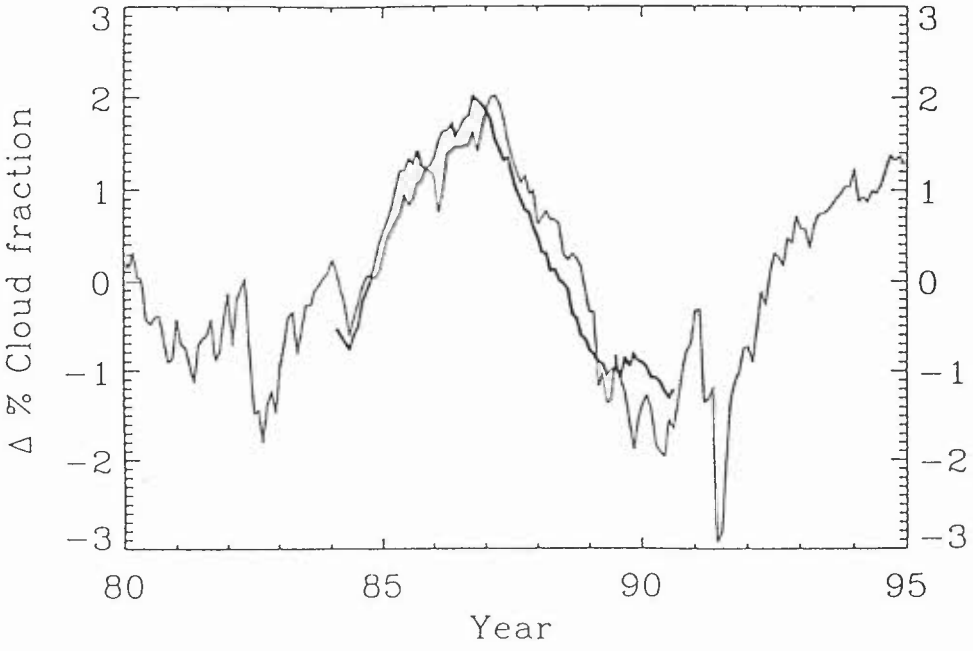

Figure 4.1 The thick curve displays the 12 months running average of cloud cover given as changes in per cent (ISCCP–C2 monthly data). The data are from the area over the oceans covered by geostationary satellites. The end points of the ISCCP–C2 curve (first and last 6 points) have been discarded. The thin curve represents the normalized monthly mean counting rate of cosmic ray intensity from Climax, Colorado, drawn to the same scale. (From Svensmark & Friis-Christensen, 1997.)

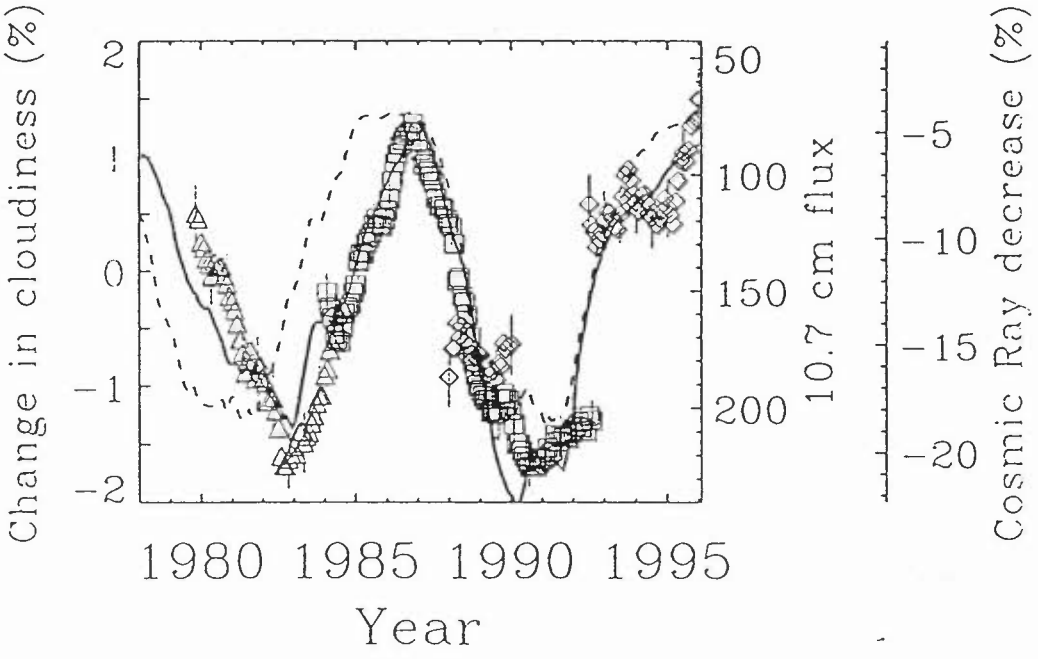

Figure 4.2 Composite figure showing changes in Earth's cloud cover from four satellite cloud data sets together with cosmic ray fluxes from Climax (solid curve, normalized to May 1965) and 10.7 cm solar flux (dashed curve, in units of 10^{-22} Wm^{-2} Hz^{-1}). Triangles are the NIMBUS-7 data, squares are the ISCCP–C2 and ISCCP–D2 data, diamonds are the DMSP data. All of the displayed data have been smoothed using a 12 month running mean. The NIMBUS-7 data are for the southern hemisphere over oceans with the tropics excluded. The DMSP data are total cloud cover for the Southern Hemisphere over oceans, and finally the ISCCP data have been derived from geostationary satellites over oceans with the tropics excluded. Also shown are 2-standard-deviation error bars for the three data sets, one for each 6 months. (From Svensmark, 1998.)

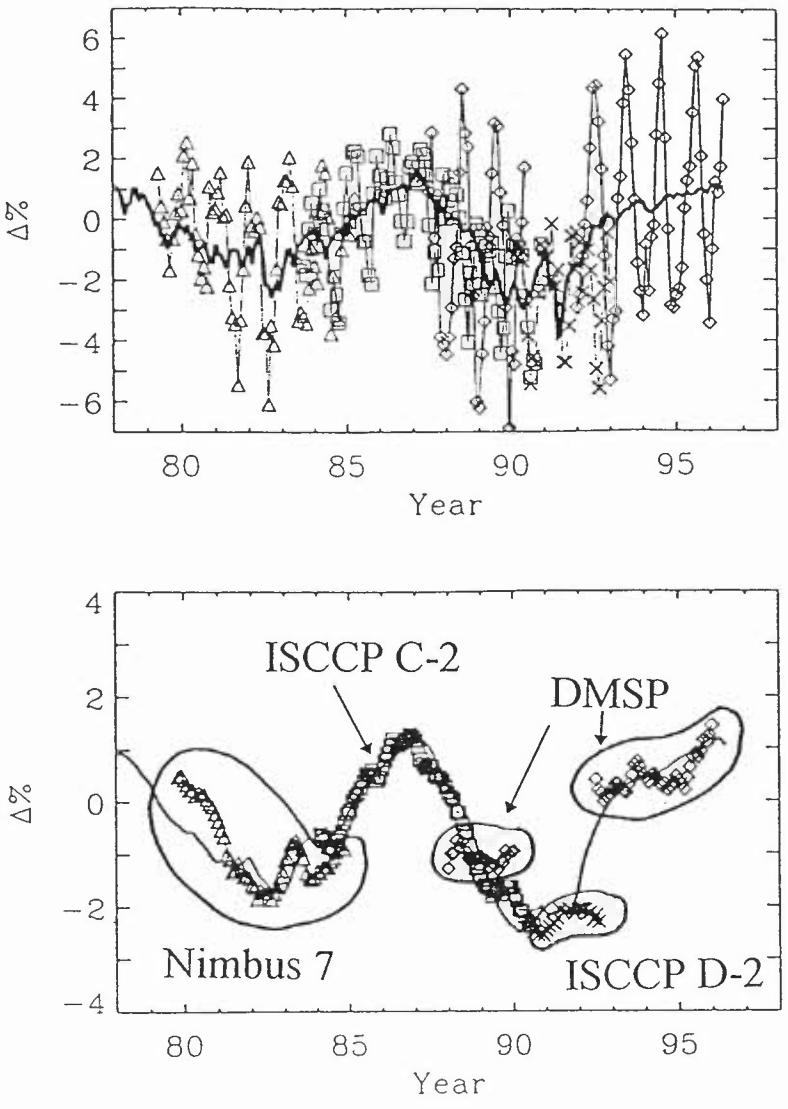

Figure 4.3 Composite figure showing four satellite cloud data sets and normalized cosmic ray fluxes from Climax (thick curve). Triangles are the NIMBUS-7 data, squares are the ISCCP–C2 data, diamonds are the DMSP data, and crosses are the ISCCP–D2 data. The top panel of the monthly values illustrates the noise level in the cloud sets. The bottom panel displays the data smoothed using a 12 month running mean. The NIMBUS-7 and the DMSP data are total cloud cover for the Southern Hemisphere over oceans, and the ISCCP data have been derived from the geostationary satellites over oceans with the tropics excluded. (From Svensmark & Friis-Christensen, 1997, annotated by KPS.)

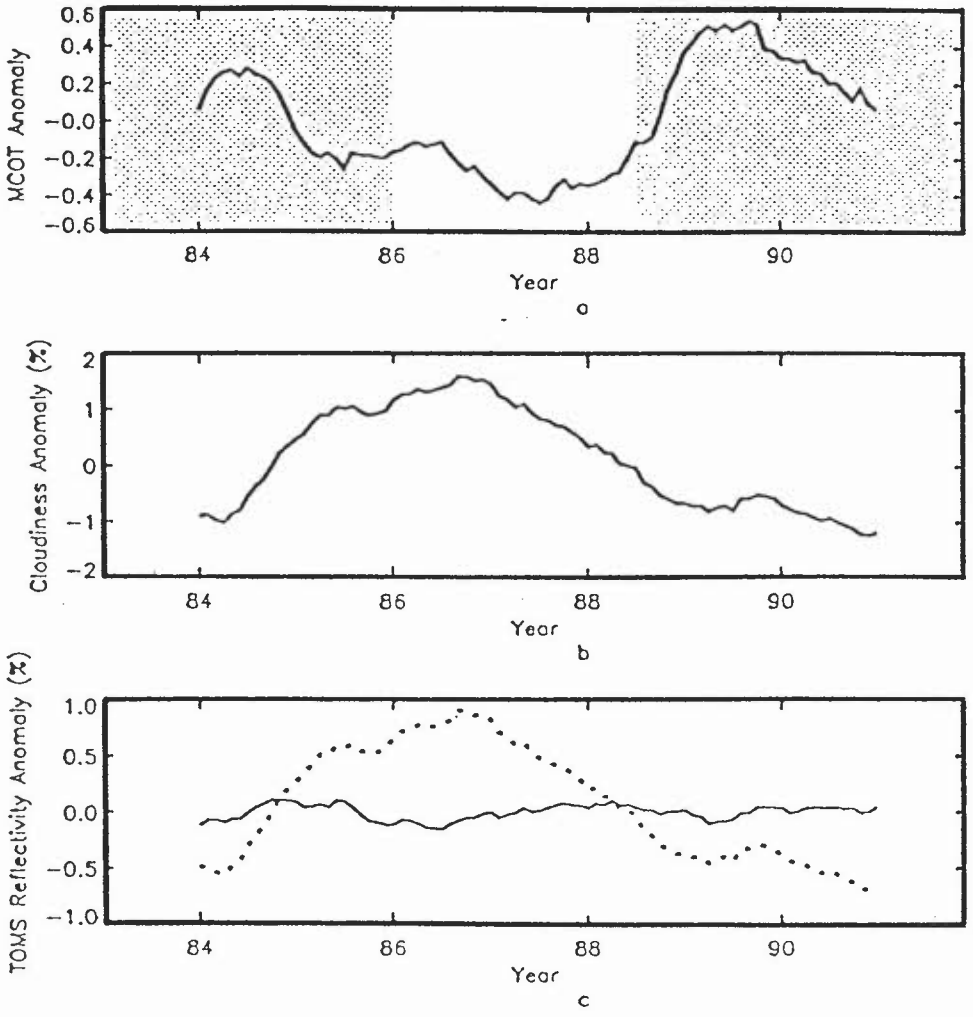

Figure 4.4 Secular variations of (a) ISCCP Mean Cloud (Visible) Optical Thickness, (b) ISCCP global cloudiness, (c) TOMS reflectivity. Dotted line in (c) is the estimated reflectivity variation caused by the global cloudiness variation given in (b). The secular variations are obtained by applying twelve month running mean after removing the mean annual cycle. The unshaded region in (a) is the time period during which the calibration problem is not significant. (From Kuang et al., 1998.)

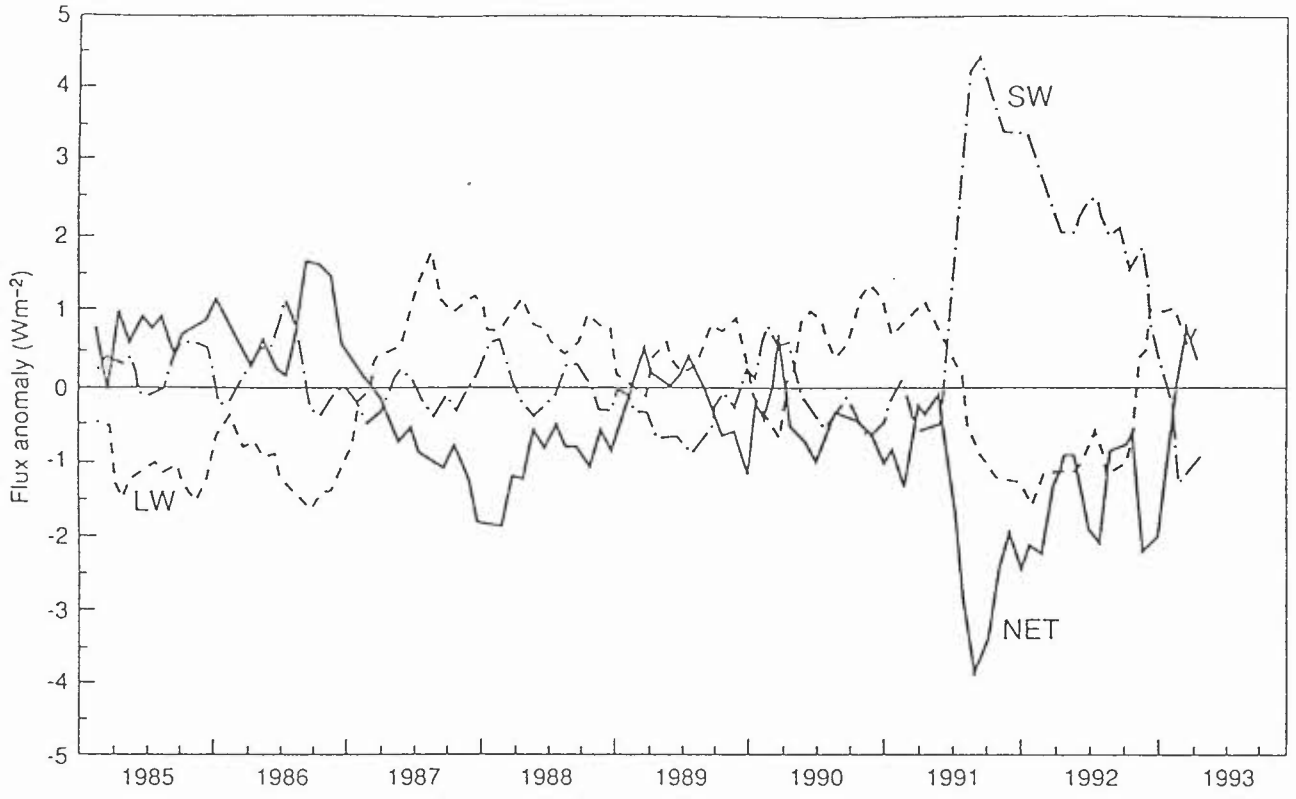

Figure 4.5 Time series of smoothed wide field of view Earth Radiation Budget Experiment long-wave (LW), short-wave (SW) and net (LW-SW) irradiance anomalies (in Wm^{-2}) between 40°N and 40°S relative to the 5 year (1985-1989) monthly mean (after Minnis et al., 1993, updated by Minnis, 1994). The deviation starting in mid-1991 is mainly due to the Mt. Pinatubo eruption – the net anomaly in August (about –4 Wm^{-2}) is almost three times higher than the standard deviation computed between 1985 and 1989. (From IPCC, 1994.)

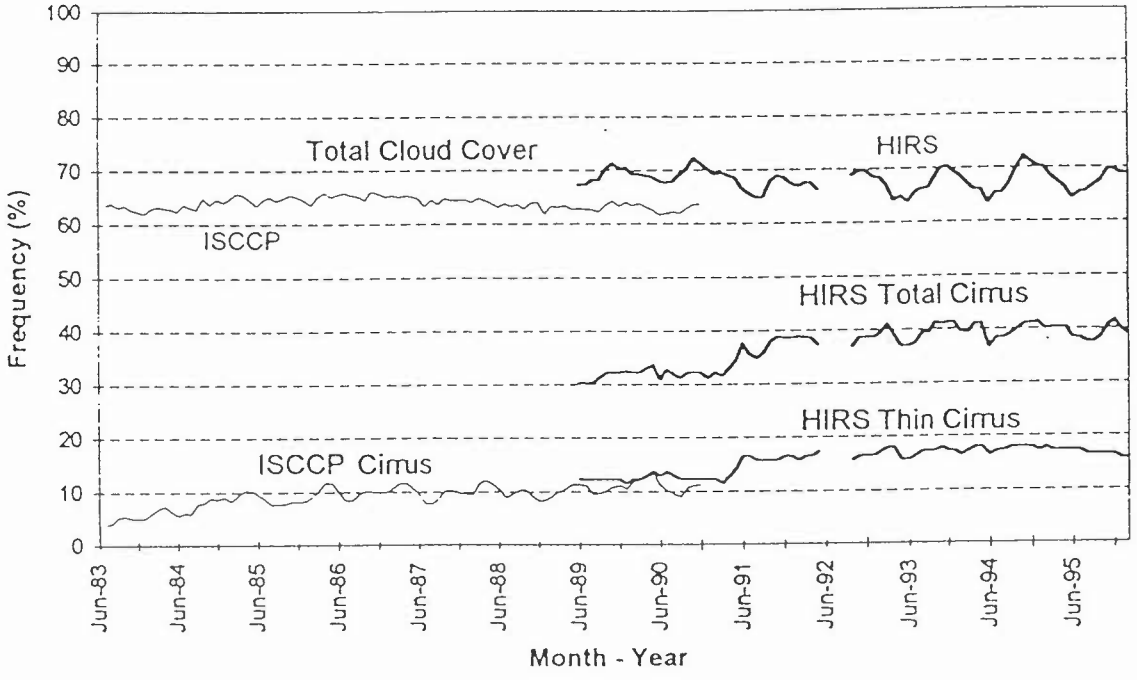

Figure 4.6 Monthly trends for ISCCP total cloud cover and cirrus (thin lines) and HIRS total cloud cover, thin cirrus, and thin plus thick cirrus (thick lines) from 1983 through 1996. (From Menzel et al., 1997.)

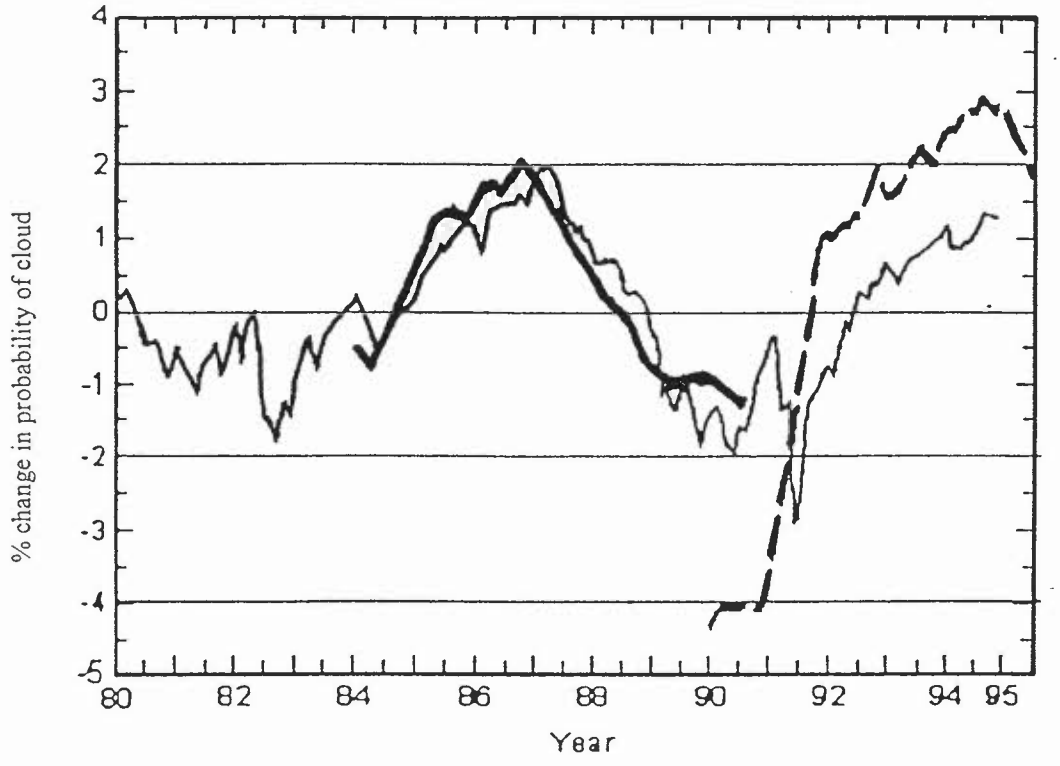

Figure 4.7 Percentage change in monthly mean cosmic ray intensity detected at Climax, CO (thin solid line) versus percentage change in twelve month running average of HIRS cirrus from 1990 to 1996 (thick dashed line). Percentage change in ISCCP twelve month running average of total cloud cover from 1984 to 1991 is also shown (thick solid line). (From Menzel et al., 1997.)

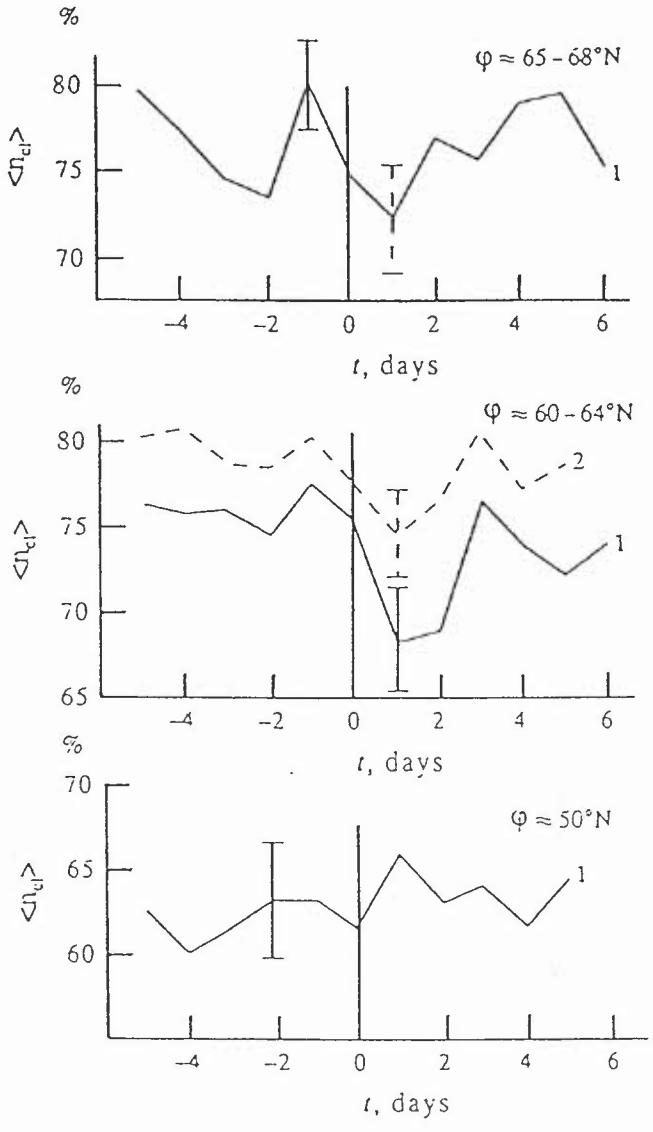

Figure 4.8 Mean variations of the total cloud cover within the different latitudinal belts in the course of Forbush-decreases of galactic cosmic ray flux. Day $t = 0$ corresponds to the day of Forbush-decrease onset. The value of cloud cover $< n_{ct} >$ is expressed as a percentage of the total sky area. Curve 1: winter events ($N = 42$). Curve 2: summer events ($N = 21$). (From Pudovkin & Veretenenko, 1995.)

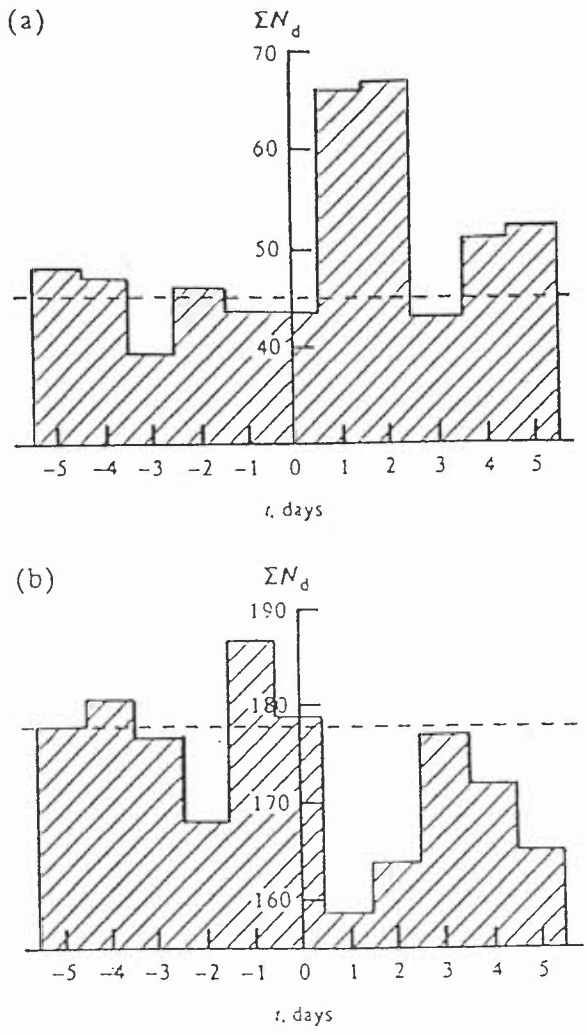

Figure 4.9 Summary number of days with clear sky (a) and with cloudy sky (b) at noon observed at the stations in the latitudinal belt $\varphi \approx 60\text{-}64°N$ during the winter Forbush-decreases. The "quiet" day level obtained by averaging over 5 days preceding the Forbush-decrease onset is shown by the dashed line. (from Pudovkin & Veretenenko, 1995.)

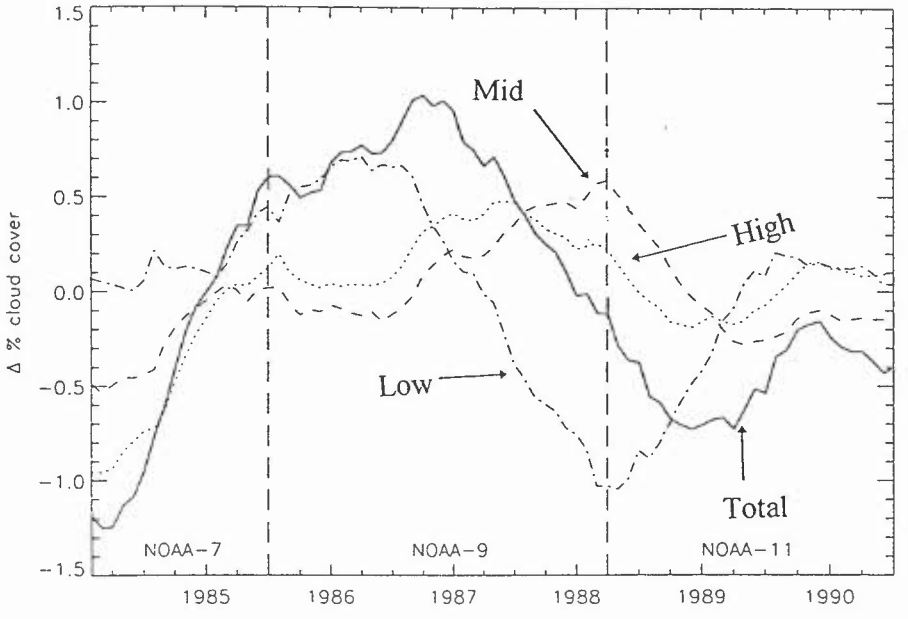

Figure 4.10 Anomalies, relative to the February 1984 – July 1990 mean, of twelve-month averaged total percentage cloud cover, and the high, mid and low level cloud components. The vertical dashed lines indicated the period within which the ISCCP calibration is believed to be most robust. (From Kernthaler et al., 1999.)

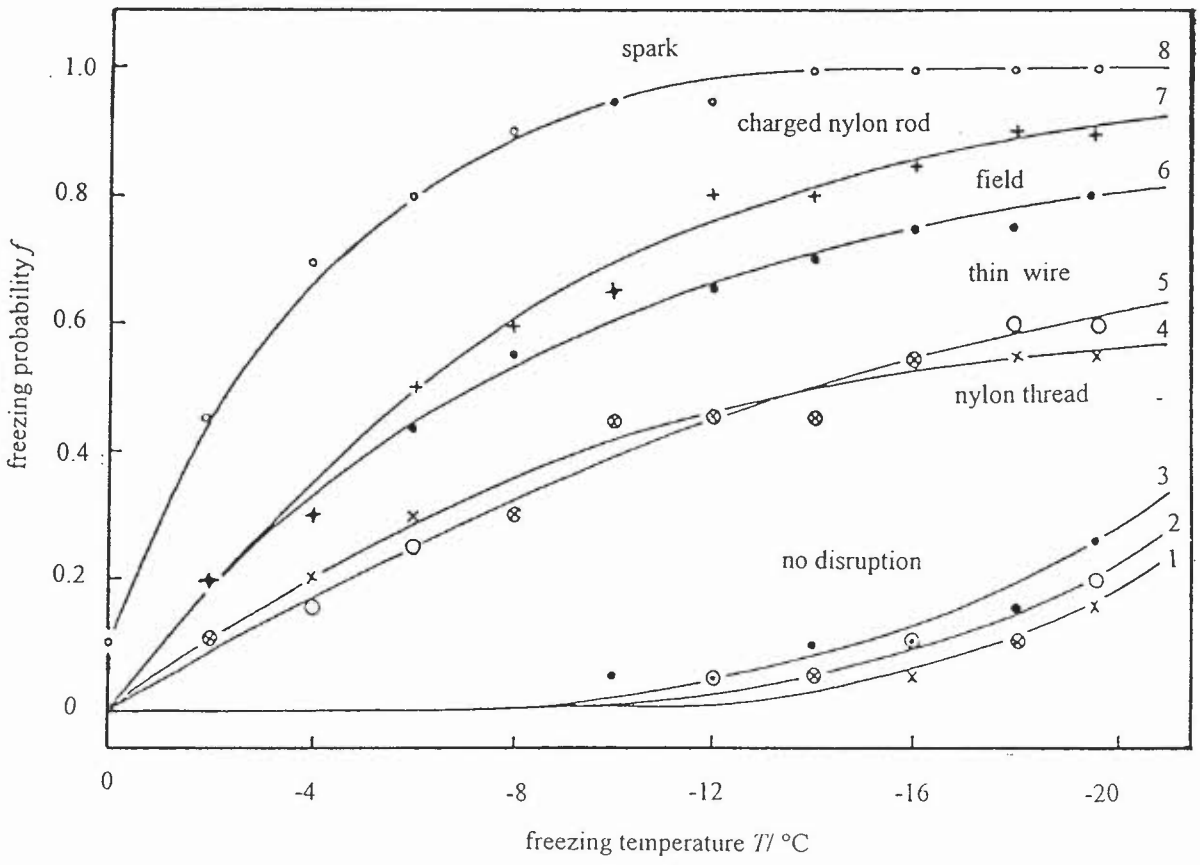

Figure 5.1 The probability of freezing f of repeated experiments on supercooled water drops of radius 1.06mm for different mechanical and electrical disruptions. Curves 1,2 and 3 are the freezing probabilities for drops undergoing no disruption, curves 4 and 5 are mechanical disruptions with nylon thread and thin wire respectively and curves 6, 7 and 8 are electrical disruptions with an electric field, a charged nylon rod and a spark respectively. (from Abbas and Latham, 1969.)

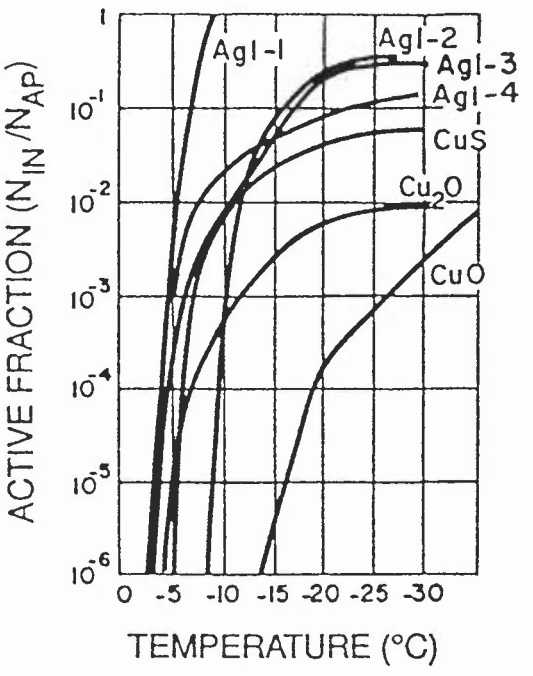

Figure 5.2 Temperature dependence of fraction of active particles as ice nuclei for various substances: AgI-1: radius 2μm, freezing mode; AgI-2: radius 0.015 to 0.2 μm (median 0.045 μm), freezing mode; AgI-3: radius 0.2 to 4 μm, deposition mode at water saturation; AgI-4: radius 2 μm, deposition mode at water saturation. (From Pruppacher and Klett, 1997)

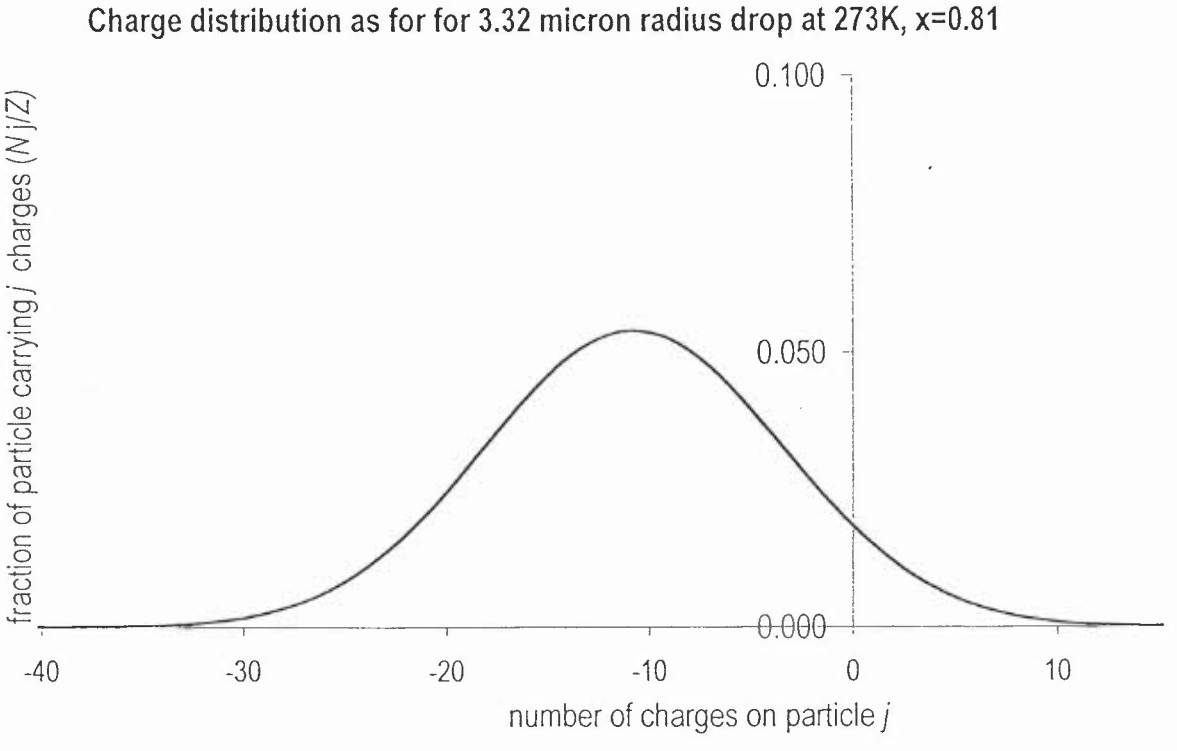

Figure 5.3 The modified Boltzmann charge distribution on 3.32μm radii drop, after Clement and Harrison (1992).

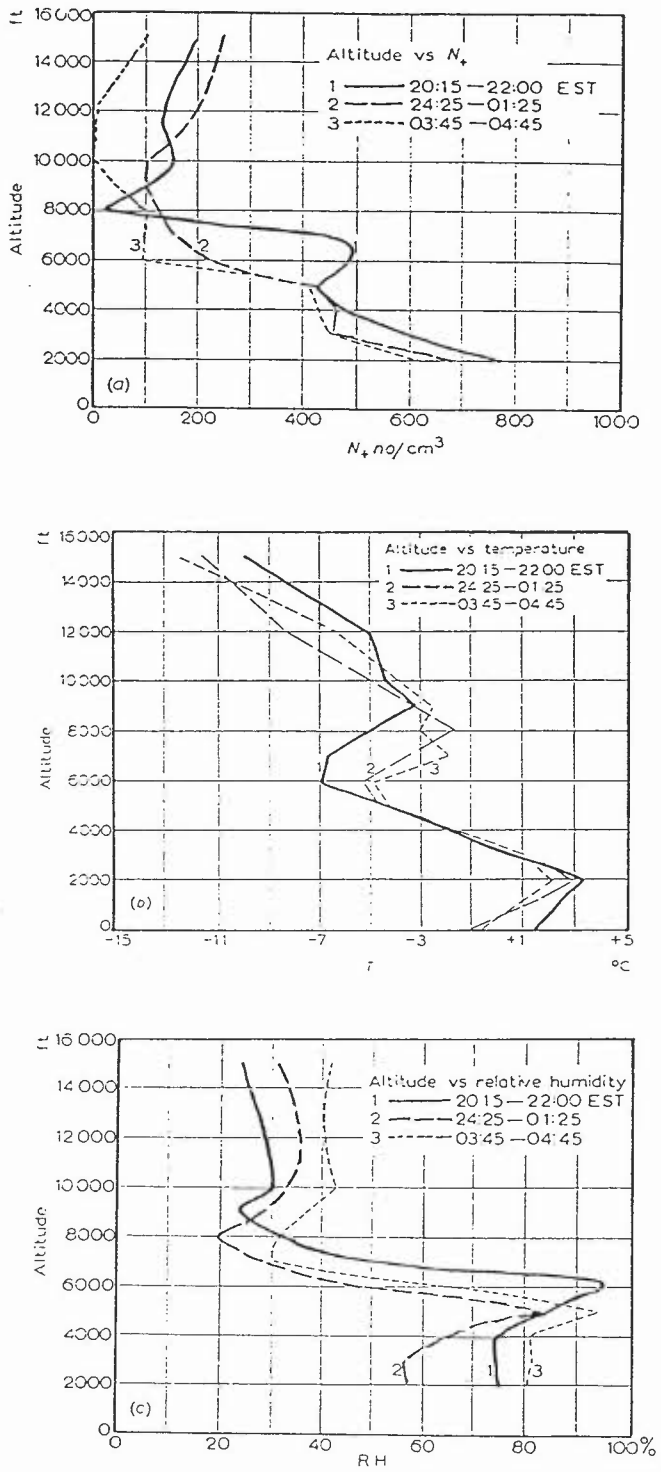

Figure 5.4 (a) Positive ion concentrations sampled as a function of altitude and time in southern New Hampshire, November 10-11 1953 by Sagalyn and Faucher (1955). (b) and (c) show the corresponding temperature and relative humidity soundings respectively.

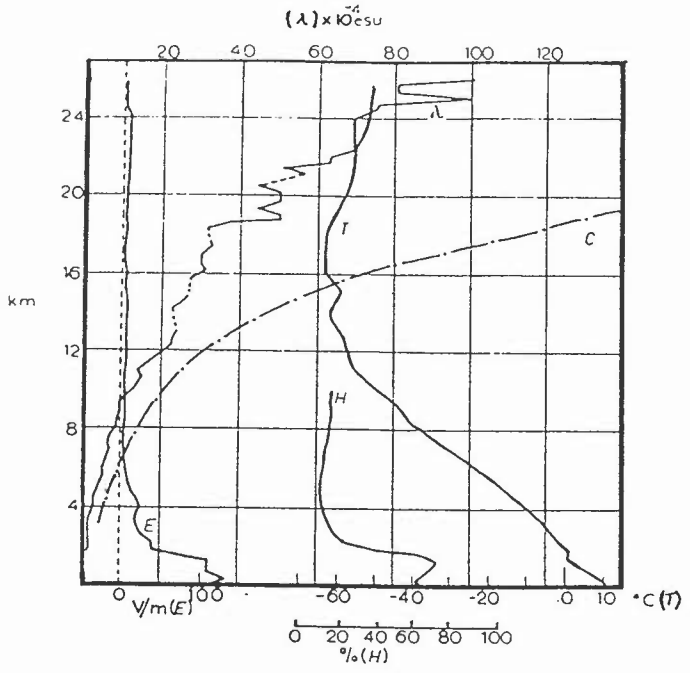

Figure 5.5 Vertical sounding of clear air atmospheric electrical properties at Hachijojima at 0300h local time on 17th December 1957 using a modified meteorological radiosonde (from Hatakeyama et al., 1958). λ is the air conductivity (directly proportional to the negative ion number concentration), E the potential gradient, C a theoretical calculation of the conductivity, T the temperature and H the relative humidity.

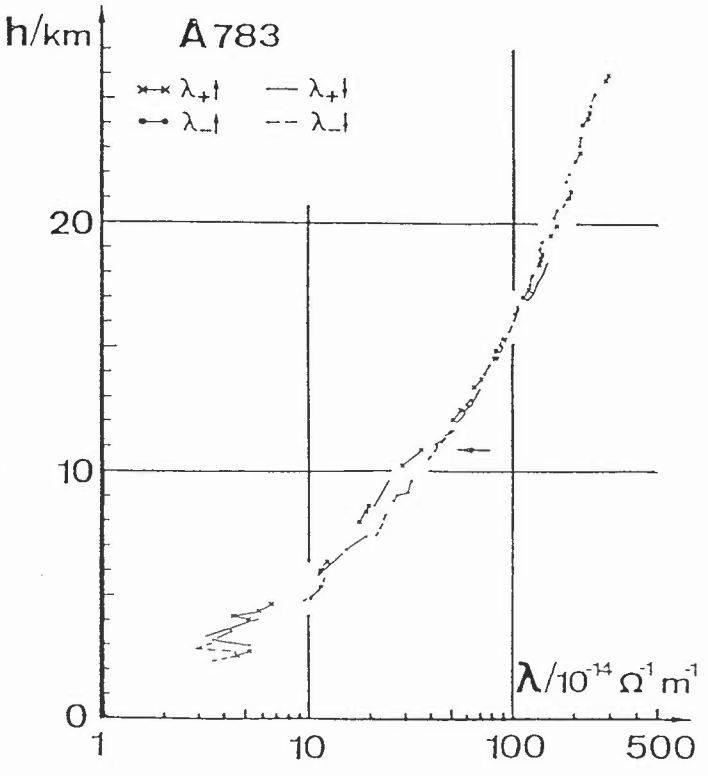

Figure 5.6 Positive and negative air conductivities (λ_+ and λ_-) during ascent and descent of a sonde reported by Gringel (1978). The arrow marks the derived height of the tropopause.

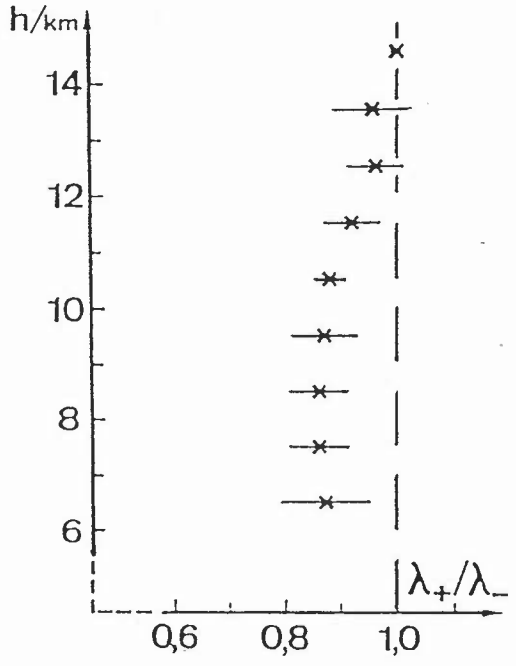

Figure 5.7 Averaged ion asymmetry ratio x determined from ten balloon ascents (Gringel, 1978), although the conductivities were always determined sequentially and not simultaneously.

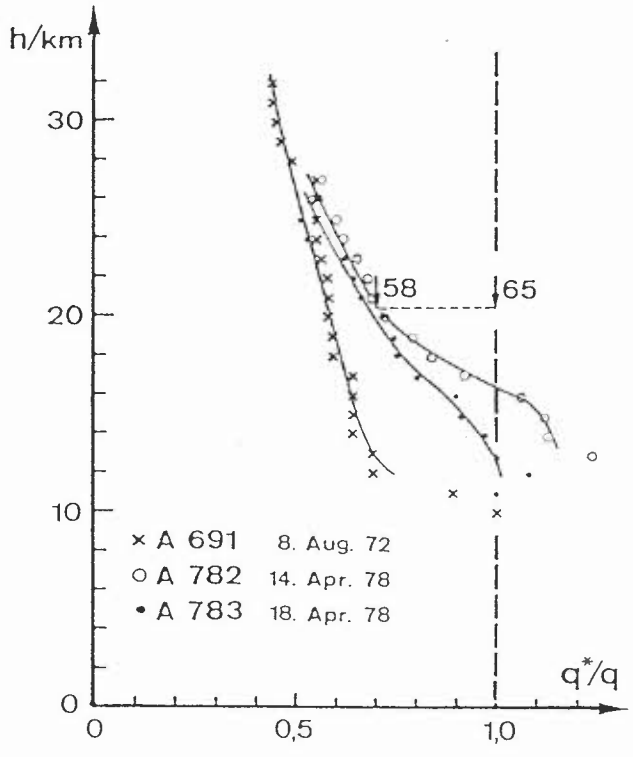

Figure 5.8 The variation of ionisation rate q^*/q in the upper atmosphere during the solar cycle found by radiosonde determination (Gringel, 1978). The arrows show the variations found between 1958 and 1965 at 50°N.

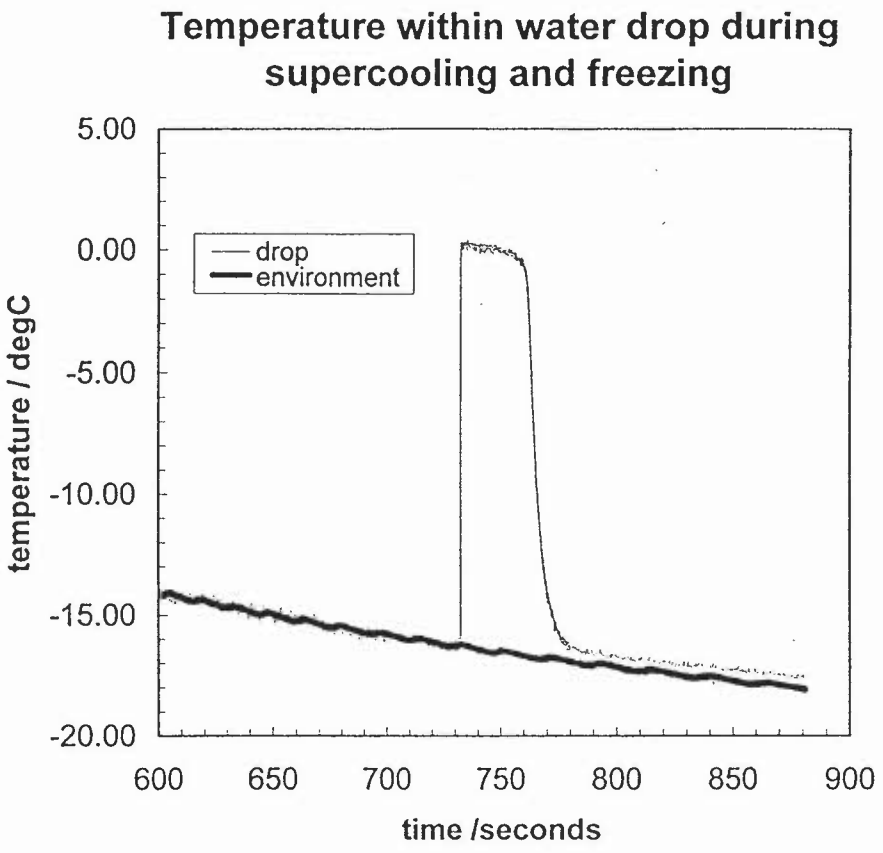

Figure 5.9 Latent heat released by a supercooled water drop at the instant of freezing (from Harrison and Lodge, 1998). On freezing the temperature of the cooled drop rises from the environmental temperature to 0°C, where it remains until all the latent heat is released and it begins to cool.